Dilution Method for Measurements of Unsteady Discharges in Mountain Streams

February 1992

D.G. Meijer

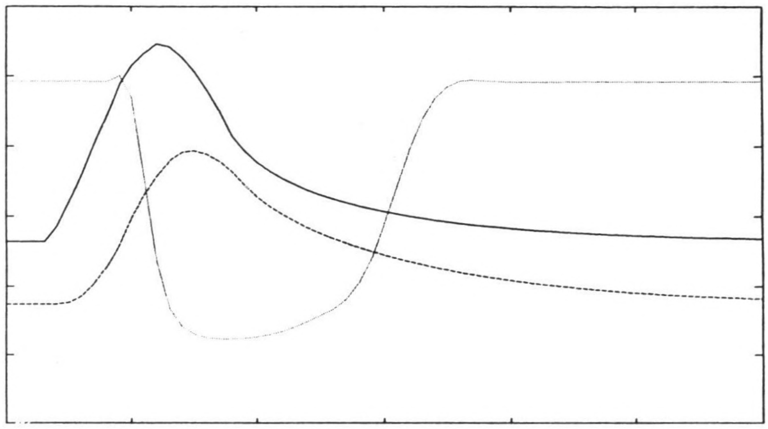

TU Delft
Delft University of Technology

Faculty of Civil Engineering
Hydraulic and Geotechnical Engineering Division
Hydraulic Engineering Group

Dilution Method

for

Measurements of Unsteady Discharges

in

Mountain Streams

D.G. Meijer

February 1992

Delft University of Technology
Faculty of Civil Engineering
Hydraulic and Geotechnical Engineering Division
Hydraulic Engineering Group

Preface

This report contains the results of my thesis written in fulfilment of my studies at the Faculty of Civil Engineering, Delft University of Technology.
The project which focuses on the determination of river discharges in mountain streams using dilution measurements, was a great challenge from both a theoretical and a practical point of view. I tried to pay attention to the theoretical (and numerical) description of flow and transport processes, as well as to the practical applicability of the suggested method.
Results, based on measurements, depend highly on the quality of the field work. In this respect, my work at ITS in Surabaya (East Java, Indonesia) was an enriching experience.
I wish to express my gratitude to my thesis supervisors prof.dr.ir. M. de Vries, dr.ir. H.L. Fontijn and dr.ir. Z.B. Wang for their support and valuable suggestions. Also to Miss ir. Anggrahini M.Sc., who made my stay in Surabaya possible, I am much obliged.

D.G. Meijer
Delft, February 1992

Table of contents

1. Introduction

In river engineering problems information on discharges and water levels is essential for many reasons. For irrigation and drinking water purposes it is very important to know how much water can be extracted from a river. Managers of waste water stations need to know how much they can release without exceeding the norms, and information on flood waves in the past help to predict the probability of flood waves in the future. Discharge measurements are therefore necessary.

Different methods to measure a river discharge exist, such as the velocity area method, the moving boat method and methods using structures like flumes and weirs. Another method is the dilution method, based on the dilution of a soluble, non-disintegrating substance, to be released in the river. For steady flows, the principles of this method are rather simple, and recommendations on how to perform the measurements already exist (ISO Handbook). However, for unsteady flows, this method is much more complicated, and even its applicability is questionable.

Studies on this topic, in which rivers were schematised as prismatic channels have already been carried out. In the present study the practice is the central issue. The applicability of the dilution method is investigated for mountain rivers with irregular cross-sections, big rocks and unsteady discharges.

In chapter 2 the principles of the dilution method are explained, and the studies made thus far are outlined, as well as the approach in the present study.
In chapter 3 the basic equations for the motion of water and transport processes, necessary for a transport model that can deal with the typical problems of an irregularly shaped mountain river, are formulated.
A numerical scheme is derived in chapter 4, resulting into a flow-and-transport-simulating computer program (FATS). Dilution discharge measurements are simulated in imaginary rivers under flood wave conditions. The river discharge is then a time dependent upstream boundary condition, and a few measurements (water levels, concentrations) are generated.
In chapter 5 a numerical procedure is developed (FINDQ) to compute the upstream river discharge, which uses only these measurements without any further information on characteristic river parameters. Determination of these parameters is an identification problem, which is solved using the DUD procedure.
The quality of the discharge determination can be estimated by comparing the result with the original upstream boundary condition in FATS, supposed to be 'true'.
Finally, in chapter 6, attention is paid to the field work and equipment required to obtain real measurements for the discharge determination. Using the FINDQ-DUD algorithm, the river discharge as a function of time can then be computed to a certain degree of accuracy, which is the eventual aim of this study.

2. Dilution discharge measurements

2.1 Dilution method for steady flow

2.1.1 Theory

A tracer (for example a salt solution) is continuously injected into a river and diluted by the flow. Downstream from the injection point the tracer concentration is measured.

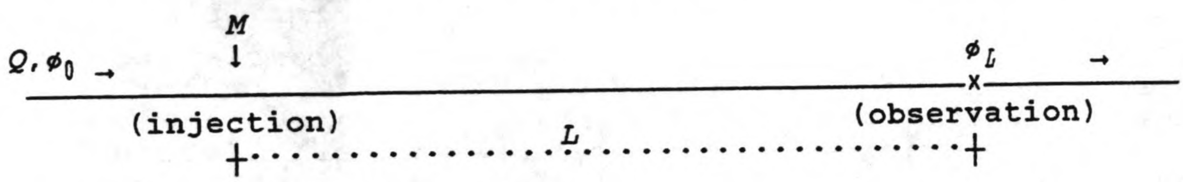

Q = river discharge [m^3/s]
ϕ_0 = (background) concentration [kg/m^3] i.e. [g/l]
M = tracer release [kg/s]
ϕ_L = measured concentration at observation point [kg/m^3]
L = mixing length [m]

fig. 2.1 Dilution method during steady discharge

The river discharge can now be calculated using the mass balance of the tracer:

$$Q = \frac{M}{\phi_L - \phi_0} \tag{2.1}$$

The distance between the injection point and the observation point is of great importance to the mixing of the tracer over the cross-section.
For the mixing length the following is recommended (ISO 1983):

$$L = 0.13\,K\,\frac{B^2}{a} \tag{2.2}$$

$$K = \frac{C(0.7C + 2\sqrt{g})}{g} \tag{2.3}$$

with: K = dimensionless dispersion coefficient [-]
B = average width [m]
a = average depth [m]
C = Chézy coefficient [$\sqrt{m}/s$]
g = acceleration due to gravity [m/s^2]

The choice of the released tracer quantity M is of great importance to the accuracy of the calculated discharge. This can be explained, by an analysis of the propagation of errors.

Generally:

With respect to sums ($c=a+b$) and substractions ($c=a-b$), the propagation of errors is presented by:

$$\sigma_c^2 = \sigma_a^2 + \sigma_b^2 \tag{2.4}$$

$$r_c^2 = \frac{a^2 r_a^2 + b^2 r_b^2}{c^2} \tag{2.5}$$

With respect to multiplications ($c=a \cdot b$) and divisions ($c=a/b$), the propagation of errors is likewise given by:

$$\sigma_c^2 = \frac{b^2\sigma_a^2 + a^2\sigma_b^2}{c^2} \tag{2.6}$$

$$r_c^2 = r_a^2 + r_b^2 \tag{2.7}$$

with:
σ = standard deviation
μ = average (expected) value
r = relative deviation ($r=\sigma/\mu$)

In these equations a subscript indicates the variable referred to. Using (2.4) through (2.7) it can be derived that the relative deviation of the computed discharge in (2.1) is found by:

$$r_Q^2 = r_M^2 + \frac{\phi_L^2\, r_{\phi_L}^2 + \phi_0^2\, r_{\phi_0}^2}{(\phi_L - \phi_0)^2} \tag{2.8}$$

Assuming a relative deviation in the equipment that measures the concentrations ($r_\phi = r_{\phi_0} = r_{\phi_L}$), (2.8) becomes:

$$r_Q^2 = r_M^2 + r_\phi^2\, \frac{\phi_L^2 + \phi_0^2}{(\phi_L - \phi_0)^2} \tag{2.9}$$

The division (last term of equation 2.9) is very significant to the accuracy of the computed discharge Q.
In the case of relatively clean water ($\phi_0 = 0$ or $\phi_0 \ll \phi_L$), the term tends to unity, and the deviation r_Q remains limited. But if ϕ_L tends to ϕ_0, r_Q becomes excessively large, which makes the measurement worthless.
This means that the release M should be chosen not too small (for $\phi_L - \phi_0 = M/Q$). On the other hand, it is desirable to keep the environmental pollution caused by the salt release within reasonable limits.

2.1.2 Practice

Two measurements were carried out as described above in the River Grindulu in East Java (Indonesia), on different days. The location was chosen in the upper reach, where the river is still a small brook.
The mixing length could not be determined by equation 2.2, because the brook was too irregularly shaped to determine geometrical parameters such as depth *a*, width *B* and Chézy-coefficient *C*. Through trial-and-error the distance, at which the concentration was practically constant was found ($L \approx 20$ m). The adaptation time was about two minutes.

fig. 2.2 Filling of the Mariotte Vessel

fig. 2.3 Direct concentration measurement

The release was performed by means of a Mariotte Vessel, filled with a NaCl solution (5%), releasing a constant discharge. The concentrations (background, at the observation point and in the vessel) were determined using a conductivity meter.

The salt concentration and the electrical conductivity of a solution are nearly linearly related. The discharge was computed by equation 2.2. In order to check the results, a velocity area test was carried out, using a current meter. The differences were respectively 9.1% on the first day, and 6.5% on the second day. However it is difficult to determine which of both methods is more accurate, these results are considered satisfactory.

2.2 Dilution method for unsteady flow

2.2.1 Introduction

Discharge measurements are especially interesting during flood wave conditions. However, some difficulties show up using the dilution method.

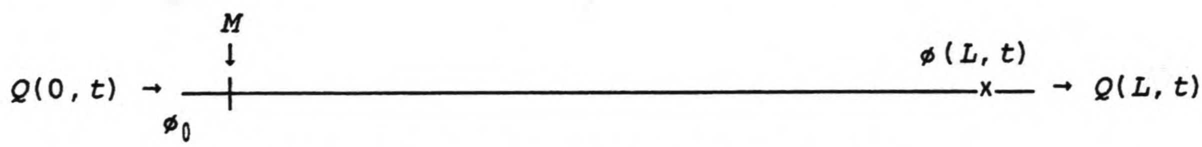

fig. 2.4 Dilution method during flood wave

It is not very easy to predict how the measured concentration $\phi(L,t)$ depends on the discharge $Q(0,t)$ or even $Q(L,t)$. The adaptation time is not given, since the situation is continuously changing. Phase shifts are to be expected. Longitudinal dispersion is now a disturbing 'spreader' of information, and dead zones have a damping effect on changing concentrations.
It is clear that equation 2.1 is not valid anymore. A dynamic flow and transport model is necessary now.
In the following, previous studies and their results are outlined, and the approach in this project is explained.

2.2.2 Noppeney's approach

Noppeney (1987) described the transport processes by a one-dimensional model based on the differential equations:

$$\frac{\partial u}{\partial t} + u\frac{\partial u}{\partial x} + g\frac{\partial a}{\partial x} - g\cdot i_b + g\frac{u^2}{C^2 a} = 0 \qquad (2.10)$$

$$\frac{\partial a}{\partial t} + u\frac{\partial a}{\partial x} + a\frac{\partial u}{\partial x} = 0 \qquad (2.11)$$

$$\frac{\partial \phi}{\partial t} + u\frac{\partial \phi}{\partial x} - K\frac{\partial^2 \phi}{\partial x^2} = 0 \qquad (2.12)$$

with: u = flow velocity [m/s]
a = depth [m]
ϕ = tracer concentration [kg/m^3]
C = Chézy coefficient [$\sqrt{m}$/s]
K = dispersion coefficient [m^2/s]
i_b = bottom slope [-]

Equations 2.10 and 2.11 represent the flow process for a prismatic channel, i.e. constant values for width B, bottom slope i_b and Chézy coefficient C. The convection and dispersion process is described by equation 2.12, in which the dispersion coefficient K can be chosen constant, or a function of the flow velocity u.

A flood-wave discharge was inserted as an upstream boundary condition $Q(0,t)$. A second upstream boundary condition was the release of the tracer M. The downstream boundary condition was the formula of Jones, which gives a $Q(h)$ relation:

$$Q = Q(h, \frac{\partial h}{\partial t}) \tag{2.13}$$

This model presented a simulation of the dilution method in a prismatic channel. The downstream concentration, calculated by this model, was considered a continuous measurement $\phi(L,t)$.
The validity of equation 2.1 was investigated. To this aim the 'measured' discharge was considered a continuous measurement:

$$Q_m = Q_m(L,t) = \frac{M}{\phi(L,t)} \tag{2.14}$$

although this is theoretically incorrect. The discharge, calculated by the flow model, was considered to be the 'true' value:

$$Q_r = Q(L,t) \tag{2.15}$$

In order to learn about the error caused by using the steady flow formula (2.1), Q_m was compared with Q_r.

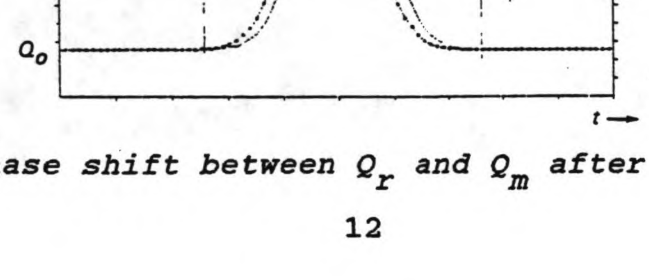

fig. 2.3 Phase shift between Q_r and Q_m after Noppeney (1987)

Noppeney found that the main error is a phase shift, caused by the difference between the flow velocity u, and the wave propagation velocity c. Since $c \approx 1.5 \cdot u$ (or $u \approx 0.67 \cdot c$), the 'information carrier' u drops behind with regard to c.

2.2.3 Vroege's approach

Vroege (1991) used an existing computer model (DUFLOW) to simulate a non-stationary river flow, and created an own model to simulate the transport processes using the results from DUFLOW. The convection and dispersion equation was extended with dead zones:

DUFLOW $\rightarrow$ $u(x,t)$ required in (2.16)

$$\frac{\partial \phi}{\partial t} + u\frac{\partial \phi}{\partial x} - K\frac{\partial^2 \phi}{\partial x^2} + D_s(\phi - \phi_d) = 0 \tag{2.16}$$

$$\frac{\partial \phi_d}{\partial t} - D_d(\phi - \phi_d) = 0 \tag{2.17}$$

with: ϕ_d = concentration in dead zone [kg/m^3]
D_d, D_s = entrainment coefficients [s^{-1}]

Dead zones contain almost stagnant water, in which the tracer can be trapped. Its concentration ϕ_d slowly adapts to the flow concentration ϕ. The entrainment coefficients D_s and D_d quantify the exchange between the main stream and the dead zones.

Vroege simulated, like Noppeney, flood waves by this 'truth' model, and generated concentration measurements $\phi(L,t)$ at the downstream boundary.
But, instead of using equation 2.1, a numerical algorithm was developed to calculate the upstream discharge $Q(0,t)$ based on the measurements $\phi(L,t)$.
Therefore the convection-dispersion model was inverted to a back-into-time (b-i-t) mode. A Kalman filtering procedure improved the results based on the measurements, and ensured stability of the backward calculation. River parameters were supposed to be known.
Initially the b-i-t model used the 'true' velocities $u(x,t)$, computed by Duflow. Since in reality, these velocities are unknown, the procedure was extended avoiding the use of these data:

1. First estimation of velocity distribution $u(x,t)$
2. Computation of $\phi(0,t)$ by b-i-t model using velocities $u(x,t)$ and measurements $\phi(L,t)$
3. Computation of discharge at upstream boundary by: $Q(0,t) = M/\{\phi(0,t) - \phi_0\}$
4. Computation of new velocity distribution by DUFLOW using $Q(0,t)$ as an upstream boundary condition with known river parameters.
5. Return to step 2

Vroege showed that this iteration procedure converges. The phase shift of Noppeney was avoided. The original upstream boundary $Q(0,t)$ of the 'true' model was approached satisfactorily; a procedure to compute the discharge based on dilution measurements was created.

However, this approach is very theoretical, and the practical applicability is questionable. The flow model DUFLOW is based on prismatic channels and requires river parameters, and cannot deal with the specific problems of irregular boulder-studded mountain rivers with undefinable river parameters.

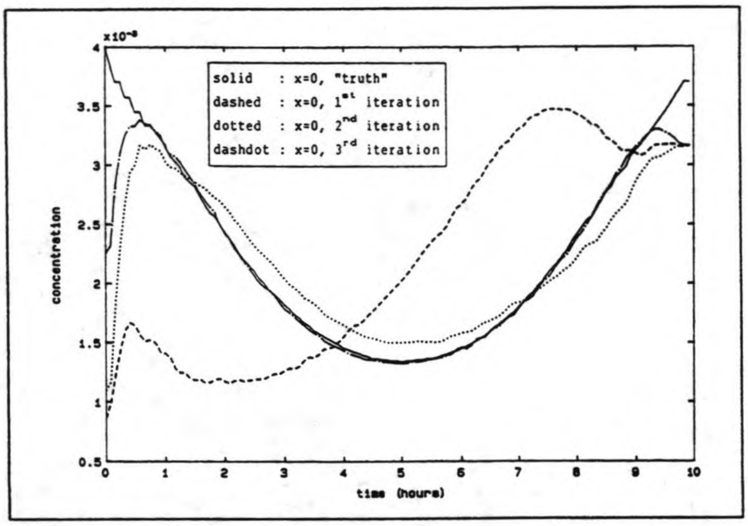

fig. 2.4 Iteration with a 6-hour flood wave (Vroege '91)

2.2.4 Approach in present study

In this study, the applicability of dilution discharge measurements in mountain streams is the central issue. Mountain streams have mostly very irregular shapes, with big rocks, high turbulence and dead zones. Geometrical parameters such as depth, width, bottom slope and bottom roughness are extremely time and place dependent, or even undefinable. Flow velocities are distributed irregularly in the longitudinal direction, throughout each cross-section, and in time.

Much attention is paid to a flow model that can deal with these problems. A one-dimensional computer model (FATS) is developed to simulate the flow and transport processes taking place. This model is used to simulate dilution measurements during flood-wave conditions in imaginary mountain rivers. Measurements are generated: the waterlevels $h(0,t)$ and $h(L,t)$, and the downstream tracer concentration $\phi(L,t)$.
A procedure is developed (computer program FINDQ) to compute the river discharge $Q(0,t)$ using only these measurements, the constant background concentration ϕ_0 and the tracer release M. No further knowledge about the river parameters is required.

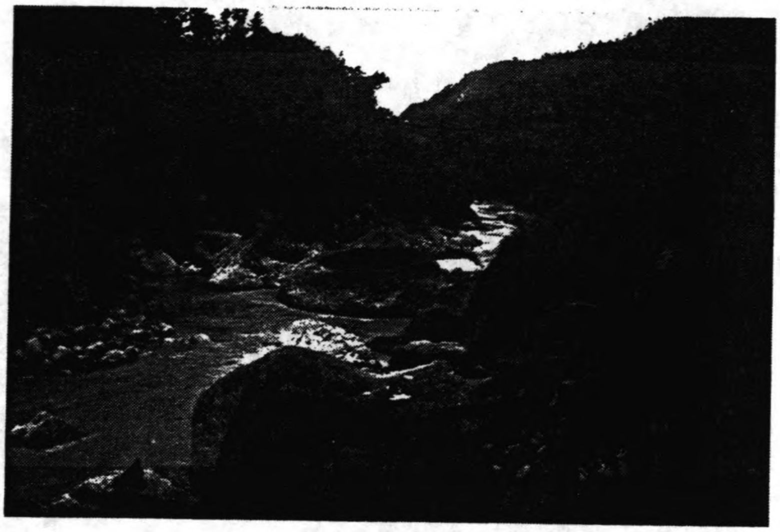

fig. 2.5 A mountain river (Grindulu, East Java)

The computer program evaluates the measurements, estimates the river parameters and reconstructs the flood wave. If an upstream river discharge and a set of river parameters can be found that yield results equal to the measurements, then one can have confidence in the determined river discharge.
This is an identification problem which is solved by a procedure called DUD which executes a few parameter improvement iterations.

Finally, attention is paid to the field work device, required to obtain the measurements.

3. *Flow and transport equations*

3.1 Introduction

In transport processes the flowing water is the carrier of the transported substance. The water movement influences the convection and dispersion of the dissolved substance, but the dissolvant does not influence the water movement (no density currents).

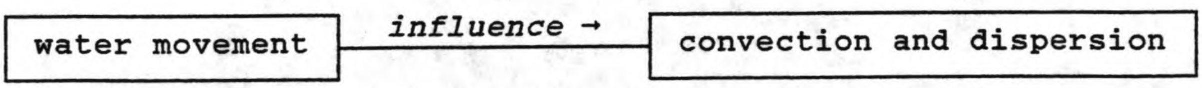

fig. 3.1 Diagram of transport process

In the transport model of this study, the flow model and the convection-dispersion model are initially separated. Later on they are merged into a model describing transport processes in rivers.

3.2 Flow processes

3.2.1 Introduction

One-dimensional unsteady flow is usually described by two differential equations based on the conservation of mass and momentum, respectively.
These equations are derived below, resulting into a continuity equation and an equation of motion, suitable to describe flow processes in mountain rivers. Typical problems such as irregular shapes, unconstant values for bottom slope, width, depth and thus cross-sectional area, undefinable roughness and turbulent velocity distribution make many usual simplifications impossible.
The fundamental principles of the motion of water are outlined. For a better understanding, the basic equations for a two dimensional vertical model (2DV-model) are derived.

3.2.2 Conservation of mass

An elementary volume of water (fig. 3.2) is taken into consideration. Its dimensions are dx and dz. The horizontal velocity component is u. The vertical component is w.

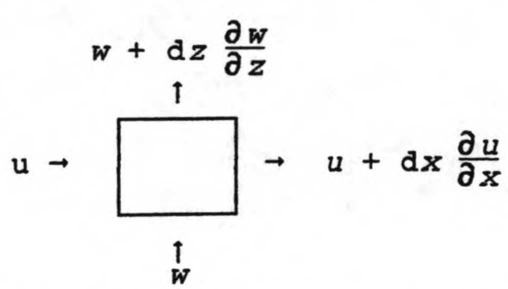

fig. 3.2 Velocity components in a water particle

The net inflow should be zero (water is supposed to be uncompressible). This yields:

$$\frac{\partial u}{\partial x} + \frac{\partial w}{\partial z} = 0 \tag{3.1}$$

3.2.3 Conservation of momentum

The stresses on an elementary volume are:

- convective stresses ρu^2, ρw^2 and ρuw
- pressure p
- shear stress τ_{xz}
- gravitation force per unit of surface $\rho g dz$

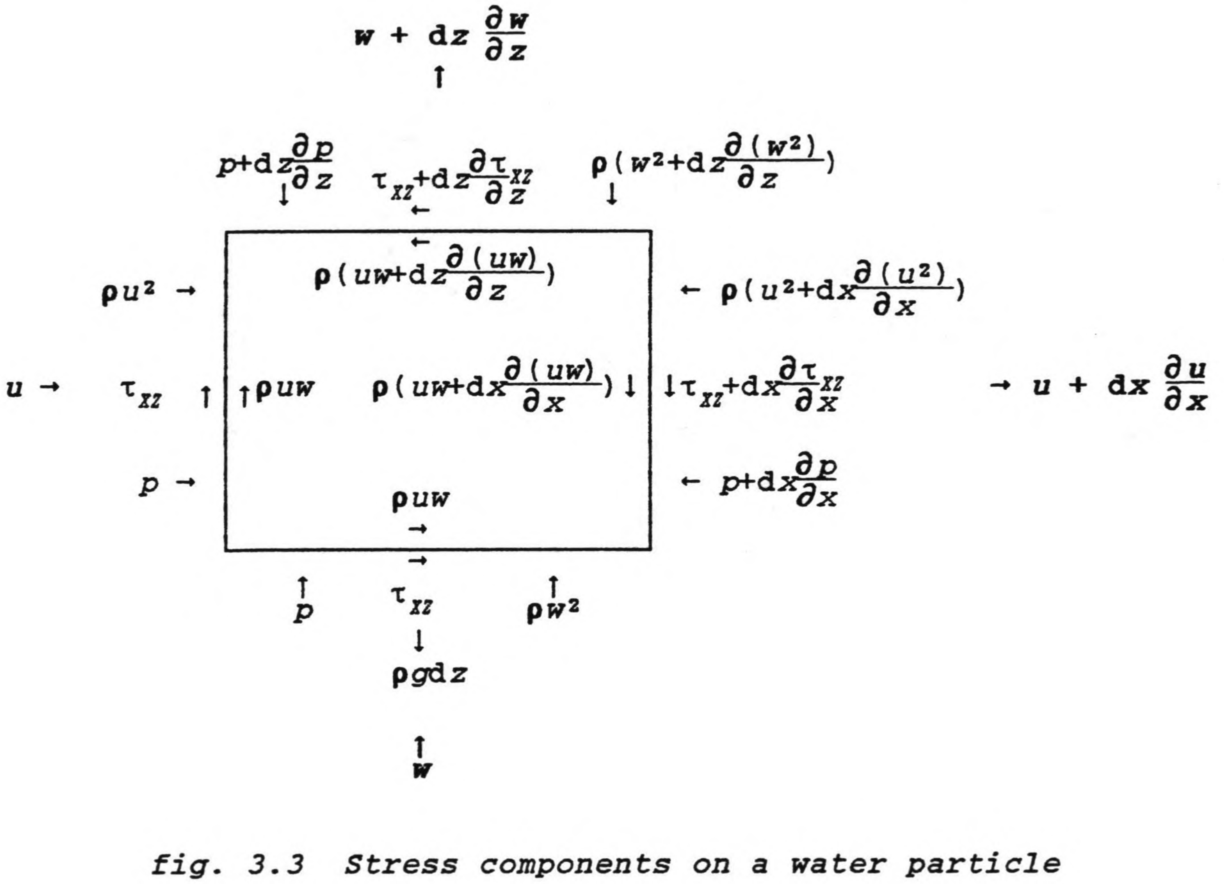

fig. 3.3 Stress components on a water particle

The acceleration components of the water particle can be found by the resulting forces:

$$\frac{\partial u}{\partial t} + \frac{\partial (u^2)}{\partial x} + \frac{\partial (uw)}{\partial z} + \frac{1}{\rho}\frac{\partial p}{\partial x} + \frac{1}{\rho}\frac{\partial \tau_{xz}}{\partial z} = 0 \tag{3.2}$$

$$\frac{\partial w}{\partial t} + \frac{\partial (uw)}{\partial x} + \frac{\partial (w^2)}{\partial z} + \frac{1}{\rho}\frac{\partial \tau_{xz}}{\partial x} + \frac{1}{\rho}\frac{\partial p}{\partial z} + g = 0 \tag{3.3}$$

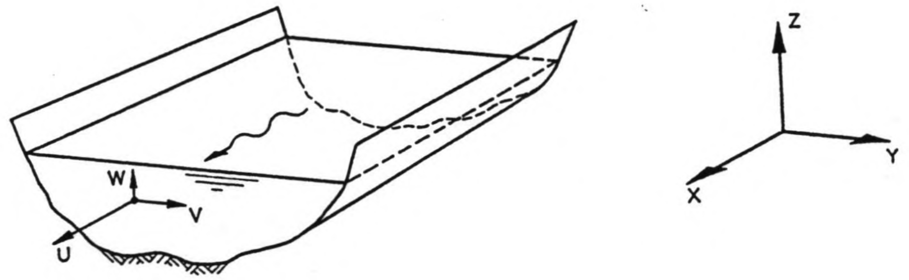

fig. 3.4 Co-ordinate system of 3D-model

Equations (3.1), (3.2) and (3.3) represent the 2DV-flow model. In a similar way the three dimensional (3D) equations can be determined:

$$\frac{\partial u}{\partial x} + \frac{\partial v}{\partial y} + \frac{\partial w}{\partial z} = 0 \tag{3.4}$$

$$\frac{\partial u}{\partial t} + \frac{\partial (u^2)}{\partial x} + \frac{\partial (uv)}{\partial y} + \frac{\partial (uw)}{\partial z} + \frac{1}{\rho}\frac{\partial p}{\partial x} + \frac{1}{\rho}\frac{\partial \tau_{xy}}{\partial y} + \frac{1}{\rho}\frac{\partial \tau_{xz}}{\partial z} = 0 \tag{3.5}$$

$$\frac{\partial v}{\partial t} + \frac{\partial (uv)}{\partial x} + \frac{\partial (v^2)}{\partial y} + \frac{\partial (vw)}{\partial z} + \frac{1}{\rho}\frac{\partial \tau_{xy}}{\partial x} + \frac{1}{\rho}\frac{\partial p}{\partial y} + \frac{1}{\rho}\frac{\partial \tau_{yz}}{\partial z} = 0 \tag{3.6}$$

$$\frac{\partial w}{\partial t} + \frac{\partial (uw)}{\partial x} + \frac{\partial (vw)}{\partial y} + \frac{\partial (w^2)}{\partial z} + \frac{1}{\rho}\frac{\partial \tau_{xz}}{\partial x} + \frac{1}{\rho}\frac{\partial \tau_{yz}}{\partial y} + \frac{1}{\rho}\frac{\partial p}{\partial z} + g = 0 \tag{3.7}$$

The local velocities consist of a time-averaged part and a fluctuation caused by turbulence:

$$U = u + u' \tag{3.8}$$

$$V = v + v' \tag{3.9}$$

$$W = w + w' \tag{3.10}$$

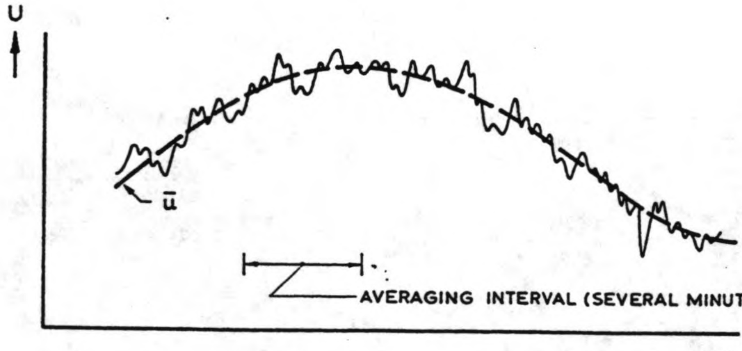

fig. 3.5 Averaging of turbulent fluctuations

The shear stresses are caused by turbulence and velocity gradients. They are defined as follows:

$$\tau_{xy} = \rho \cdot \overline{u'v'} - \rho\nu\frac{\partial u}{\partial y} = \rho \cdot \overline{u'v'} - \rho\nu\frac{\partial v}{\partial x} \tag{3.11}$$

$$\tau_{xz} = \rho \cdot \overline{u'w'} - \rho\nu\frac{\partial u}{\partial z} = \rho \cdot \overline{u'w'} - \rho\nu\frac{\partial w}{\partial x} \tag{3.12}$$

$$\tau_{yz} = \rho \cdot \overline{v'w'} - \rho\nu\frac{\partial v}{\partial z} = \rho \cdot \overline{v'w'} - \rho\nu\frac{\partial w}{\partial y} \tag{3.13}$$

in which ν is the kinematic viscosity of water.

3.2.4 Integration over the cross-section

In order to obtain a one-dimensional flow model, the equations (3.4 through 3.7) have to be integrated over the cross-section.
First, the equation of mass conservation (3.4) is integrated.

$$\iint_A \left(\frac{\partial u}{\partial x} + \frac{\partial v}{\partial y} + \frac{\partial w}{\partial z}\right) dydz = 0 \tag{3.14}$$

This integration (Jansen et al. 1979) yields the continuity equation:

$$\frac{\partial A}{\partial t} + \frac{\partial Q}{\partial x} = 0 \tag{3.15}$$

Integration of the momentum equations (3.5 through 3.7) over the cross-section can be applied in a similar way.

$$\frac{\partial}{\partial t}\iint_A u dydz + \frac{\partial}{\partial x}\iint_A u^2 dydz + \iint_A \frac{\partial}{\partial y}(uv) dydz + \iint_A \frac{\partial}{\partial z}(uw) dydz +$$

$$+ \frac{1}{\rho}\iint_A \frac{\partial p}{\partial x} dydz + \frac{1}{\rho}\iint_A \frac{\partial \tau_{xy}}{\partial y} dydz + \frac{1}{\rho}\iint_A \frac{\partial \tau_{xz}}{\partial z} dydz = 0 \tag{3.16}$$

The terms of (3.16) are analysed separately. The first integral represents the river discharge. The second integral can be written as:

$$\iint_A u^2 dydz = \alpha \overline{u}^2 A = \alpha \frac{Q^2}{A} \tag{3.17}$$

with:

$$\alpha = \frac{A}{Q^2} \iint_A u^2 \, dy dz \tag{3.18}$$

This α is the velocity distribution parameter. If the flow is uniformly distributed over the cross-section, then $\alpha=1$. If there are local deviations, then $\alpha>1$.

The third and fourth integrals of (3.16) are assumed to be zero, because the local velocities V and W in the river cross-section are close to zero. In (3.9) and (3.10) it is reasonable to assume $v=0$ and $w=0$. The local lateral velocities are then expressed by $V=v'$ and $W=w'$. Their influence is already incorporated in τ_{xy} and τ_{xz} (by 3.11 and 3.12).

The last two terms of (3.16) can be written as:

$$\frac{1}{\rho}\iint_A \left(\frac{\partial \tau_{xy}}{\partial y} + \frac{\partial \tau_{xz}}{\partial z}\right) dy dz = \frac{P \cdot \overline{\tau_b}}{\rho} \tag{3.19}$$

with:

$\overline{\tau_b}$ = mean bottom stress [N/m²]
P = wetted perimeter [m]

The meaning of these parameters P en $\overline{\tau_b}$ is that all shear stress acting on the water in the cross-section is caused by the contact with the 'fixed' boundaries.

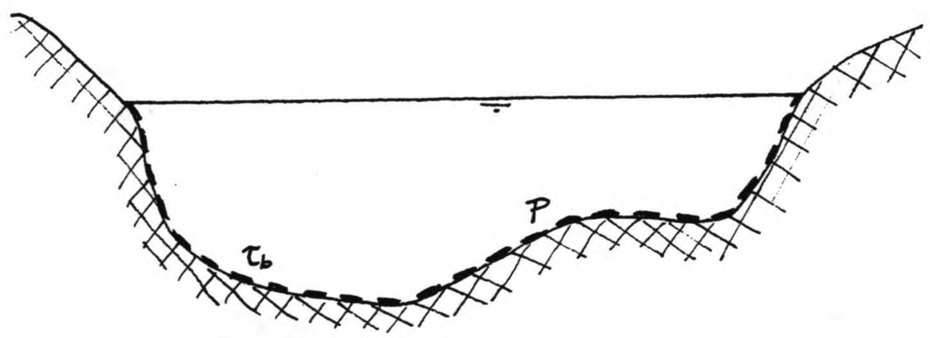

fig. 3.6 Wetted perimeter and bottom stress in a cross-section

Usually the pressure in a river cross-section (3.16, fifth term) is assumed to be hydrostatic. However, this assumption cannot be made for a turbulent mountain river, where pressure fluctuations can occur due to local accelerations.

$$p = \rho g(h-z) + p' \tag{3.20}$$

The pressure p consists of a hydrostatic term and a fluctuation p'. Its gradient is:

$$\frac{\partial p}{\partial x} = \rho g\frac{\partial h}{\partial x} + \frac{\partial p'}{\partial x} \tag{3.21}$$

The fifth term of (3.16) now becomes:

$$\frac{1}{\rho}\iint\limits_A \frac{\partial p}{\partial x}\mathrm{d}y\mathrm{d}z = g\iint\limits_A \frac{\partial h}{\partial x}\mathrm{d}y\mathrm{d}z + \frac{1}{\rho}\iint\limits_A \frac{\partial p'}{\partial x}\mathrm{d}y\mathrm{d}z = gA\frac{\partial h}{\partial x} + \frac{1}{\rho}\frac{\partial}{\partial x}(\overline{p'}A) \tag{3.22}$$

with: $\overline{p}'$= cross-sectional averaged pressure deviation [N]
h = waterlevel [m]

Substitutions of these terms into (3.16) gives:

$$\frac{\partial Q}{\partial t} + \frac{\partial}{\partial x}(\alpha\frac{Q^2}{A}) + gA\frac{\partial h}{\partial x} + \frac{1}{\rho}[\frac{\partial}{\partial x}(\overline{p'}A) + P\overline{\tau_b}] = 0 \tag{3.23}$$

This equation of motion contains terms for the acceleration, the convection, the slope of the water surface, a gradient of an averaged pressure fluctuation and a term for the bottom friction.

The continuity equation (3.15), and the equation of motion (3.23) together describe the flow process in a river under the following assumptions:

- constant values for ρ, g and ν
- no feeding or leakage by groundwater flow, rain or evaporation
- uncompressibility of water

The last two terms between brackets in (3.23) are unknown functions of x, Q and A (and A is a function of h). They can be combined in an empirical function:

$$f(x,Q,h) = \frac{1}{\rho}[\frac{\partial}{\partial x}(\overline{p'}A) + P\overline{\tau_b}] \tag{3.24}$$

It is to be expected that the bottom friction is the decisive factor.

A formula for the bottom friction exists:

$$\frac{P\tau_b}{\rho} = \frac{g}{C^2}\frac{Q|Q|}{A_s R} = \frac{gA_s}{C^2 R}u|u| \qquad (3.25)$$

with: A_s = flow cross-section [m²]
$R = A_s/P$ = hydraulic radius [m]

But this equation is based on assumptions that cannot be made, such as:

- prismatic channel
- constant Chézy parameter based on bottom roughness
- uniform velocity distribution

Therefore (3.25) is not used, and f remains an empirical, not yet determined function.

This makes the flow model:

$$\frac{\partial A}{\partial t} + \frac{\partial Q}{\partial x} = 0 \qquad (3.26)$$

$$\frac{\partial Q}{\partial t} + \frac{\partial}{\partial x}\left(\alpha\frac{Q^2}{A}\right) + gA\frac{\partial h}{\partial x} + f = 0 \qquad (3.27)$$

In this model several variables appear. Q and h are the variables to be solved. In order to make (3.26) and (3.27) well defined, the following relations must be known:

$$A = A(x,h) \qquad (3.28)$$

$$\alpha = \alpha(x,h) \qquad (3.29)$$

$$f = f(x,Q,h) \qquad (3.30)$$

3.2.4 Characteristic celereties

The fysical meaning of the characteristic celerities is the propagation speed of infinite small disturbances in the water surface.
In order to find these celerities, equations (3.26) and (3.27) are rewritten in Q and h.

$$B\frac{\partial h}{\partial t} + \frac{\partial Q}{\partial x} = 0 \qquad (3.31)$$

$$\frac{\partial Q}{\partial t} + 2\frac{\alpha Q}{A}\frac{\partial Q}{\partial x} + \left[gA - B'\left(\frac{\alpha Q}{A}\right)^2\right]\frac{\partial h}{\partial x} = -f \qquad (3.32)$$

with:

$$B' = \frac{\partial}{\partial h}\left(\frac{A}{\alpha}\right) \tag{3.33}$$

The expressions of the total differentials belonging to the system are:

$$dQ = dt\frac{\partial Q}{\partial t} + dx\frac{\partial Q}{\partial x} \tag{3.34}$$

$$dh = dt\frac{\partial h}{\partial t} + dx\frac{\partial h}{\partial x} \tag{3.35}$$

Matrix notation gives:

$$\begin{bmatrix} 0 & 1 & B & 0 \\ 1 & \frac{2\alpha Q}{A} & 0 & gA-B'\left(\frac{\alpha Q}{A}\right)^2 \\ dt & dx & 0 & 0 \\ 0 & 0 & dt & dx \end{bmatrix} \begin{bmatrix} \partial Q/\partial t \\ \partial Q/\partial x \\ \partial h/\partial t \\ \partial h/\partial x \end{bmatrix} = \begin{bmatrix} 0 \\ -f \\ dQ \\ dh \end{bmatrix} \tag{3.36}$$

The celerities are found if the system coefficient matrix equals zero (Jansen et al. 1979). This gives:

$$\left[\frac{dx}{dt}\right]^2 - 2\frac{\alpha Q}{A}\left[\frac{dx}{dt}\right] - \frac{gA}{B} + \frac{B'}{B}\left(\frac{\alpha Q}{A}\right)^2 = 0 \tag{3.37}$$

yielding:

$$c_{1,2} = \left[\frac{dx}{dt}\right]_{1,2} = \frac{\alpha Q}{A} \pm \sqrt{\frac{gA}{B} + \left(\frac{\alpha Q}{A}\right)^2\left(1 - \frac{B'}{B}\right)} \tag{3.38}$$

The sign of c represents the direction of the wave propagation.

3.2.5 Flood-wave celerity

For flood waves with a relatively long wave period, the flood wave celerity can be found using a quasi-steady flow description. Neglecting the acceleration term in the equation of motion provides a unique $Q(h)$ relation for steady flow, transformable to a $Q(A)$ relation. The continuity equation can be rewritten in Q.

$$\frac{dA}{dQ}\frac{\partial Q}{\partial t} + \frac{\partial Q}{\partial x} = 0 \tag{3.39}$$

which is the same as:

$$\frac{\partial Q}{\partial t} + \frac{dQ}{dA}\frac{\partial Q}{\partial x} = 0 \tag{3.40}$$

Recognise the simple wave structure with a propagation velocity:

$$c = \frac{dQ}{dA} \tag{3.41}$$

For two standard cases simple expressions can be found.
In the first case a constant width is considered and a uniform velocity distribution over the entire cross-section.

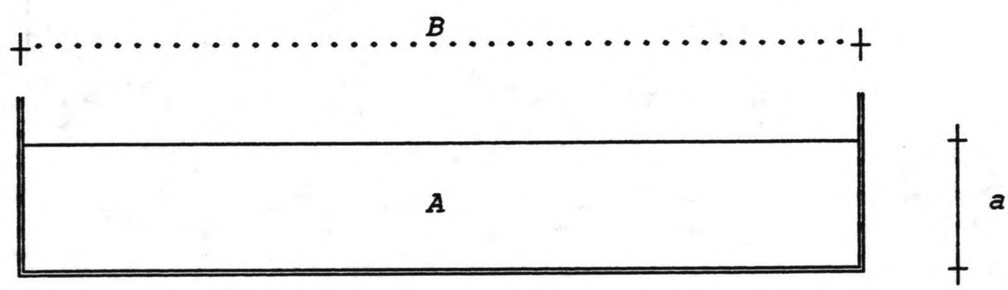

fig. 3.7 Theoretical cross-section

The discharge is given by:

$$Q = BCi^{1/2}a^{3/2} = B^{-1/2}Ci^{1/2}A^{3/2} \tag{3.42}$$

with: a = depth [m]
C = Chézy coefficient [√m/s]
i = bottom slope [-]

Its derivative to A is:

$$\frac{dQ}{dA} = \frac{3}{2}B^{-1/2}Ci^{1/2}A^{1/2} = \frac{3}{2}\frac{Q}{A} \tag{3.43}$$

which can be written as:

$$c = \frac{3}{2}u \tag{3.44}$$

In the second case, the flow area is only a part of the river cross-section.

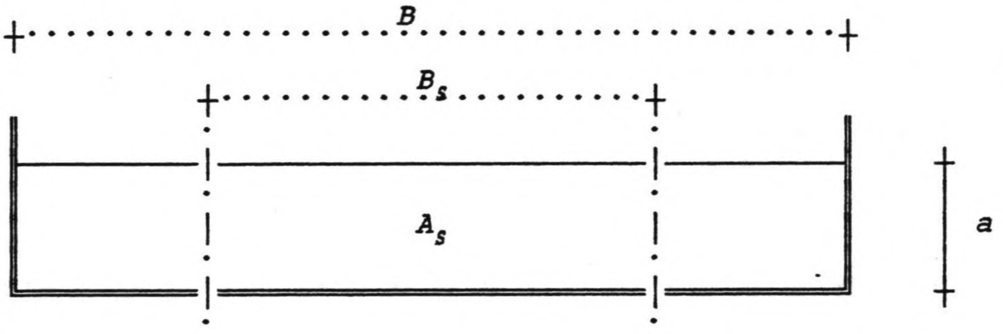

fig. 3.8 Theoretical cross-section with flow area

An example of such a cross-section is a river with groynes. The discharge is given by:

$$Q = B_s^{-1/2} C i^{1/2} A_s^{3/2} \tag{3.45}$$

Its derivative to A is:

$$\frac{dQ}{dA} = \frac{dQ}{dA_s}\frac{dA_s}{dA} = \frac{3}{2}\frac{Q}{A_s}\frac{B_s}{B} \tag{3.46}$$

yielding:

$$c = \frac{3}{2}\frac{B_s}{B}u \tag{3.47}$$

In most cases, expressions like these will not be found so easily. In streams with irregular shapes and undefinable geometrical proportions, equation (3.41) requires an empirical $Q(h)$ relation and a local river width.

$$c = \frac{dQ}{dh}\frac{dh}{dA} = \frac{1}{B}\frac{dQ}{dh} \tag{3.48}$$

which is a local value.

The propagation time over the length L is:

$$T = \int_0^L c^{-1}\, dx \tag{3.49}$$

3.3 Convection, diffusion and dispersion

3.3.1 Introduction

Convection is the longitudinal transport of a dissolved substance, caused by the stream. Meanwhile, mixing takes place in three dimensions, caused by:

- molecular diffusion
- turbulent diffusion
- dispersion

The influence of molecular diffusion is negligible with regard to turbulent diffusion and dispersion, and therefore usually not taken into account.

3.3.2 Convection and turbulent diffusion

A two-dimensional basic equation for convection and turbulent diffusion can be found by an analysis of a mass balance.

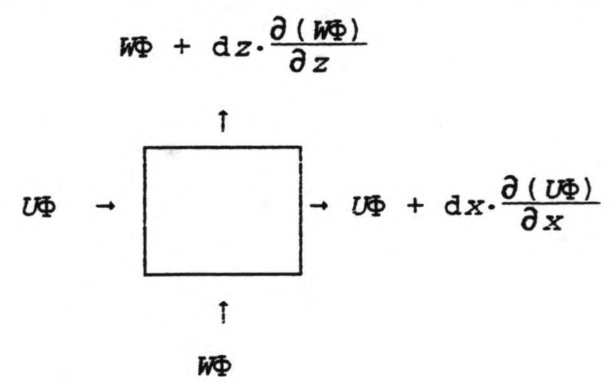

fig. 3.9 Mass flux components in an elemantary volume

A mass balance yields:

$$\frac{\partial\Phi}{\partial t} + \frac{\partial(U\Phi)}{\partial x} + \frac{\partial(W\Phi)}{\partial z} = 0 \tag{3.50}$$

On the analogy of (3.8) and (3.10) the time-averaged velocity is separated from its turbulent fluctuation (fig. 3.5). Similarly, it is defined:

$$\Phi = \phi + \phi' \tag{3.51}$$

Substitution into (3.50), and averaging over a short time interval yields:

$$\frac{\partial}{\partial t}\overline{(\phi + \phi')} + \frac{\partial}{\partial x}(\overline{u\phi} + \overline{u\phi'} + \overline{u'\phi} + \overline{u'\phi'}) +$$

$$+ \frac{\partial}{\partial z}(\overline{w\phi} + \overline{w\phi'} + \overline{w'\phi} + \overline{w'\phi'}) = 0 \tag{3.52}$$

Evaluation of the terms shows:

$\overline{\phi + \phi'} = \phi$	because $\overline{\phi'} = 0$ by definition
$\overline{u\phi} = u\phi$	convective transport
$\overline{u\phi'} = u \cdot \overline{\phi'} = 0$	because $\overline{\phi'} = 0$
$\overline{u'\phi} = \overline{u'} \cdot \phi = 0$	because $\overline{u'} = 0$ by definition

The terms $\overline{u'\phi'}$ and $\overline{w'\phi'}$ represent the turbulent diffusive transport. Taylor (1953) assumed in a one-dimensional consideration a negative linear relation between the diffusive transport and the concentration gradient.

$$\overline{u'\phi'} = -K \frac{\partial \phi}{\partial x} \tag{3.53}$$

with: K = diffusion coefficient [m^2/s]

In a two-dimensional consideration, a matrix notation gives:

$$\begin{bmatrix} \overline{u'\phi'} \\ \overline{w'\phi'} \end{bmatrix} = - \begin{bmatrix} K_{11} & K_{12} \\ K_{21} & K_{22} \end{bmatrix} \begin{bmatrix} \partial\phi/\partial x \\ \partial\phi/\partial z \end{bmatrix} \tag{3.54}$$

Assuming that the co-ordinate system is chosen in the main directions (i.e. $K_x=K_{11}$, $K_z=K_{22}$ and $K_{12}=K_{21}=0$), equation (3.52) becomes:

$$\frac{\partial \phi}{\partial t} + \frac{\partial}{\partial x}(u\phi) - \frac{\partial}{\partial x}(K_x \frac{\partial \phi}{\partial x}) + \frac{\partial}{\partial z}(w\phi) - \frac{\partial}{\partial z}(K_z \frac{\partial \phi}{\partial z}) = 0 \tag{3.55}$$

The second and fourth term of (3.55) can be replaced by:

$$\frac{\partial}{\partial x}(u\phi) + \frac{\partial}{\partial z}(w\phi) = u\frac{\partial \phi}{\partial x} + w\frac{\partial \phi}{\partial z} + \phi(\frac{\partial u}{\partial x} + \frac{\partial w}{\partial z}) \tag{3.56}$$

in which the bracketed term equals zero, satisfying the equation of conservation of mass (3.1).

Substitution, and extension to 3D-mode gives:

$$\frac{\partial \phi}{\partial t} + u\frac{\partial \phi}{\partial x} - \frac{\partial}{\partial x}(K_x \frac{\partial \phi}{\partial x}) + v\frac{\partial \phi}{\partial y} - \frac{\partial}{\partial y}(K_y \frac{\partial \phi}{\partial y}) + w\frac{\partial \phi}{\partial z} - \frac{\partial}{\partial z}(K_z \frac{\partial \phi}{\partial z}) = 0 \tag{3.57}$$

with: K_x = longitudinal diffusion coefficient
K_y = transversal diffusion coefficient
K_z = vertical diffusion coefficient

The assumption of Taylor has proven its validity in practice for turbulent diffusion. But (3.57) is only a local transport equation. In order to quantify the transport in a river, integration over the cross-section is required.

3.3.3 Dispersion

Dispersion is the effect of convection deviations over the cross-section, caused by a non-uniform velocity distribution. This is, beside turbulent diffusion, an additional 'spreader' of substance in longitudinal direction.

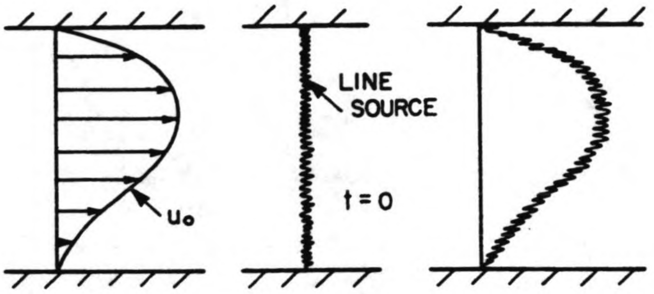

fig. 3.10 Mixing process in a river (2DH)

Again the basic continuity equation (3.50) is considered, but in a 3D-mode:

$$\frac{\partial \Phi}{\partial t} + \frac{\partial (U\Phi)}{\partial x} + \frac{\partial (V\Phi)}{\partial y} + \frac{\partial (W\Phi)}{\partial z} = 0 \qquad (3.58)$$

Integration over the cross-section gives an expression for the river transport.

$$\frac{\partial}{\partial t}\iint_A \Phi \, dy dz + \frac{\partial}{\partial x}\iint_A U\Phi \, dy dz = 0 \qquad (3.59)$$

The last two terms of (3.58) vanish, because the total lateral transport must be zero (no external source).

For U and Φ is defined:

$$U = \overline{u} + u'' \qquad (3.60)$$

$$\Phi = \overline{\phi} + \phi'' \qquad (3.61)$$

with the overbars indicating cross-sectional averaged values, and the quatation marks a local deviation.

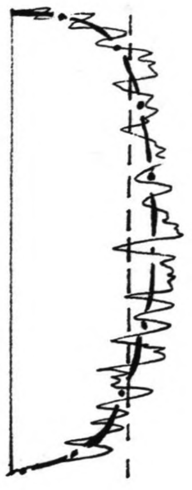

——— U = local velocity

-·-·-·- u = local time averaged velocity

u' = turbulent fluctuation

- - - - $\overline{u}$ = cross sectional averaged velocity

u'' = local deviation

$U = u + u'$ and $U = \overline{u} + u''$

fig. 3.11 Cross-sectional velocity distribution

Equation (3.59) now becomes:

$$\frac{\partial}{\partial t}\iint_A (\overline{\phi} + \phi'')\,dydz + \frac{\partial}{\partial x}\iint_A (\overline{u}\overline{\phi} + \overline{u}\phi'' + u''\overline{\phi} + u''\phi'')\,dydz = 0 \tag{3.62}$$

The integrated deviations cancel out, yielding:

$$\frac{\partial}{\partial t}(A\overline{\phi}) + \frac{\partial}{\partial x}(A\overline{u}\overline{\phi}) + \frac{\partial}{\partial x}(A\overline{u''\phi''}) = 0 \tag{3.63}$$

which can be written as:

$$A\frac{\partial\overline{\phi}}{\partial t} + \overline{\phi}\frac{\partial A}{\partial t} + \overline{\phi}\frac{\partial}{\partial x}(A\overline{u}) + A\overline{u}\frac{\partial\overline{\phi}}{\partial x} + \frac{\partial}{\partial x}(A\overline{u''\phi''}) = 0 \tag{3.64}$$

The second and third term vanish, because they satisfy the continuity equation of the water movement (3.26).

$$\overline{\phi}\left(\frac{\partial A}{\partial t} + \frac{\partial Q}{\partial x}\right) = 0 \tag{3.65}$$

Now it is assumed (see also 3.53) that the dispersive transport is negative linear to the average concentration gradient.

$$\overline{u''\phi''} = -K\frac{\partial\overline{\phi}}{\partial x} \tag{3.66}$$

with: K = longitudinal dispersion coefficient [m²/s]

Notice that this K value includes the effect of turbulent diffusion (see fig. 3.11). Although assumption (3.66) is very questionable, it is widely practised (Fischer 1979) in transport computations. This makes (3.64):

$$A\frac{\partial\overline{\phi}}{\partial t} + A\overline{u}\frac{\partial\overline{\phi}}{\partial x} - \frac{\partial}{\partial x}(AK\frac{\partial\overline{\phi}}{\partial x}) = 0 \qquad (3.67)$$

3.3.4 Example

In a river with steady flow, a constant cross-sectional area and a constant dispersion coefficient, a pollutant with mass M is instantaneously released at x=0 and t=0. Now (3.67) can be simplified to:

$$\frac{\partial\overline{\phi}}{\partial t} + \overline{u}\frac{\partial\overline{\phi}}{\partial x} - K\frac{\partial^2\overline{\phi}}{\partial x^2} = 0 \qquad (3.68)$$

An analytical solution is given by:

$$\overline{\phi}(x,t) = \frac{M/A}{2\sqrt{\pi K t}}\exp(\frac{-(x-\overline{u}t)^2}{4Kt}) \qquad (3.69)$$

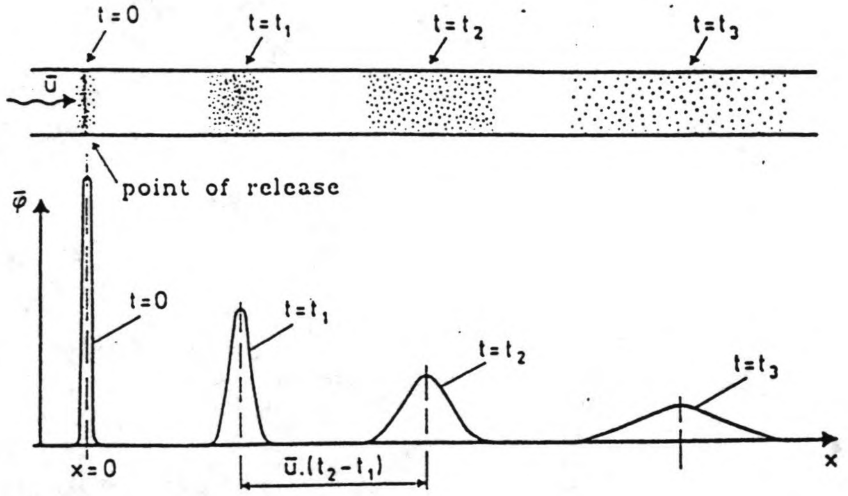

fig. 3.12 Concentration distributions after the Taylor model

This is a Gauss curve, moving forward with $\overline{u}$. The maximum concentration decreases by $t^{-1/2}$.

3.3.5 Skewness

This Gaussianity is a consequence of (3.66). However, measurements in natural streams usually show a skewness in the distribution curves. A relatively steep front and a long tail are characteristic of this skewness.
This skewness is caused by the interaction between lateral dispersion and longitudinal convection, a process more complicated than a one-dimensional transport equation can describe.

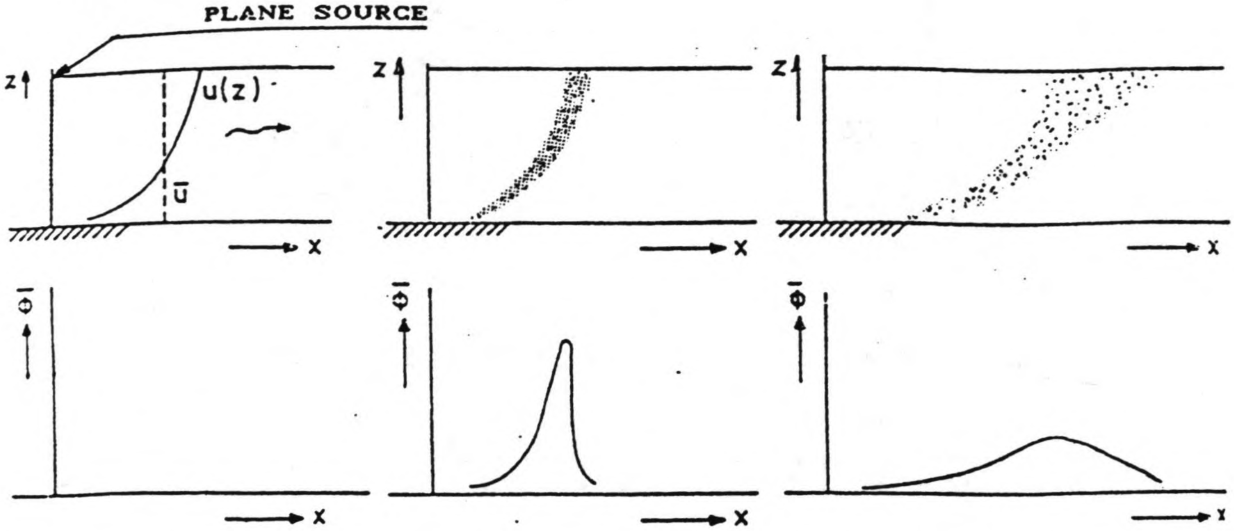

fig. 3.13 Skewness in concentration distribution (Fischer 1966)

3.3.6 Disintegration of the substance

If a pollutant disintegrates (for example biologically), its total mass decreases with time. This can be quantified by:

$$\frac{\partial M}{\partial t} = -kM \tag{3.70}$$

with: k = disintegration factor [s^{-1}]

Therefore the concentrations from $x=-\infty$ to $x=\infty$ will decrease at the same rate. For a non-conservative pollutant, (3.67) becomes:

$$A\frac{\partial\overline{\phi}}{\partial t} + A\overline{u}\frac{\partial\overline{\phi}}{\partial x} - \frac{\partial}{\partial x}(AK\frac{\partial\overline{\phi}}{\partial x}) - Ak\overline{\phi} = 0 \tag{3.71}$$

In this study, the transport of tracers in rivers is investigated. As a tracer material, a conservative substance is usually chosen. This means that k=0.

3.3.7 Dead zones

An important extension of (3.71) is the exchange of the dissolved substance between the main flow and the dead zones.

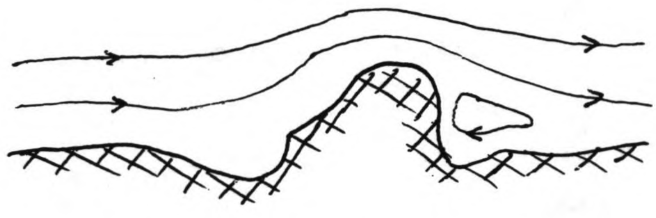

fig. 3.14 Dead zone behind a stone in a mountain river

Examples of dead zones are:

- areas behind obstacles
- areas between groynes
- an inland harbour at the river
- non-flowing water particles due to bed roughness and vegetation

Because these zones are not a part of the stream, they react more slowly to changing concentrations. For convenience the overbars will be omitted from now on.

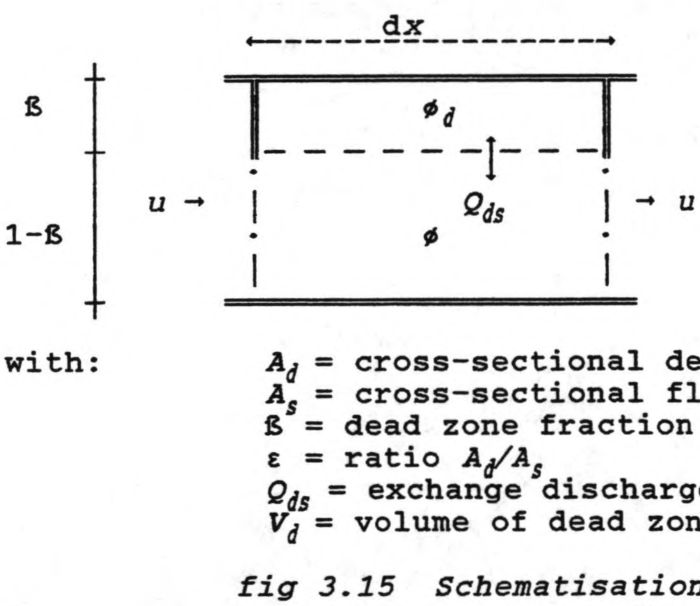

$$A_d = ßA = \varepsilon A_s$$

$$A_s = (1-ß)A$$

$$\varepsilon = \frac{ß}{1-ß}$$

with:
A_d = cross-sectional dead zone area [m²]
A_s = cross-sectional flow area [m²]
ß = dead zone fraction
ε = ratio A_d/A_s
Q_{ds} = exchange discharge [m³/s]
V_d = volume of dead zone [m³]

fig 3.15 Schematisation of a dead zone

Between the dead zone and the main stream, turbulence causes an exchange discharge Q_{ds}.

The net influx equals the storage:

$$Q_{ds}(\phi - \phi_d)\,dt = V_d \frac{\partial \phi_d}{\partial t} dt \tag{3.72}$$

which is the same as:

$$\frac{\partial \phi_d}{\partial t} - D(\phi - \phi_d) = 0 \tag{3.73}$$

with : $D = \frac{Q_{ds}}{V_d}$ = entrainment coefficient [s^{-1}]

The entrainment coefficient can be considered as the inverse of the exchange time, i.e. the time required for the dead zone to exchange its own volume.
The influence of this exchange on the concentration in the flow area is:

$$\frac{\partial \phi}{\partial t} + \varepsilon D(\phi - \phi_d) = 0 \tag{3.74}$$

The one-dimensional convection-dispersion model with dead zones is now represented by the equations:

$$\frac{\partial \phi}{\partial t} + u\frac{\partial \phi}{\partial x} - \frac{1}{A_s}\frac{\partial}{\partial x}(A_s K\frac{\partial \phi}{\partial x}) + \varepsilon D(\phi - \phi_d) = 0 \tag{3.75}$$

$$\frac{\partial \phi_d}{\partial t} - D(\phi - \phi_d) = 0 \tag{3.76}$$

Dead zones also have a skewing effect on passing concentration clouds, because they behave like internal sources. The effect of the dead zones on the skewness of the concentration distribution is of greater importance than the effect of the non-uniform velocity distribution over the cross-section.
Especially in turbulent, irregularly-shaped mountain streams the dead zones will be decisive for the skewness in the observed data.
The skewness of a concentration distribution can be quantified by the method of moments. Nordin and Troutman (1980) give a relation between skewness and physical parameters like ß, *D*, *K* and *u*.

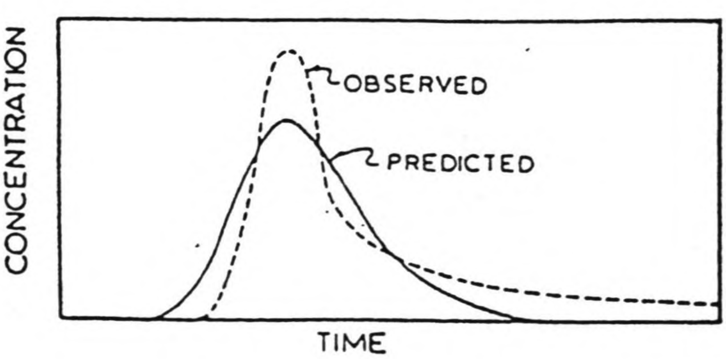

fig. 3.16 Skewness in observed data (Thackston and Schnelle 1970)

3.4 Transport model

3.4.1 Model equations

As explained in section 3.1, the combination of a flow model and a convection-dispersion model describes the transport processes of a dissolved substance in a channel.

These model equations are:

$$\left[\begin{array}{ll} \dfrac{\partial A}{\partial t} + \dfrac{\partial Q}{\partial x} = 0 & (3.77) \\[2ex] \dfrac{\partial Q}{\partial t} + \dfrac{\partial}{\partial x}(\alpha \dfrac{Q^2}{A_s}) + gA_s\dfrac{\partial h}{\partial x} + f = 0 & (3.78) \\[2ex] \dfrac{\partial \phi}{\partial t} + u\dfrac{\partial \phi}{\partial x} - \dfrac{1}{A_s}\dfrac{\partial}{\partial x}(A_s K\dfrac{\partial \phi}{\partial x}) + \varepsilon D(\phi - \phi_d) = 0 & (3.79) \\[2ex] \dfrac{\partial \phi_d}{\partial t} - D(\phi - \phi_d) = 0 & (3.80) \end{array}\right.$$

Notice the small change in (3.78) with regard to (3.27). Since the cross-section is divided into a flow area and dead zones, the equation of motion should exclude these zones and A should be replaced by A_s. The continuity equation (3.77), however, describes storage over the full cross-section A.

The symbols in the equations are recapitulated:

System variables (functions of x and t):

Q = river discharge [m^3/s]
h = water surface level with respect to reference datum [m]
ϕ = mean concentration in cross-sectional flow area [kg/m^3]
ϕ_d = mean concentration in dead zones [kg/m^3]

Physical constant

g = acceleration due to gravity ($\approx$ 9.81 m/s^2)

Interrelated parameters

geometrical functions of x and h:

A = cross-sectional area [m^2]
A_s = (1-ß)A = cross-sectional flow area [m^2]
α = velocity distribution parameter over A_s (see 3.18)
ß = dead zone fraction
ε = ratio A_b/A_s = ß/(1-ß)

flow dependent functions of x, h and Q:

f = resistance parameter [m^3/s^2]
u = Q/A_s = mean flow velocity in flow area [m/s]
K = one-dimensional dispersion coefficient [m^2/s]
D = entrainment coefficient [s^{-1}]

The influence of the irregular shape of a mountain river bed and its flow profile is expressed by these parameters. In order to make the transport model work, these parameter functions must be known.

Obviously modelling an existing river requires a huge investigation at different sites of the river in question during different discharges. However, this is not the aim of this study.

The transport model of this study is meant to model imaginary rivers with arbitrarily chosen parameters. In these imaginary rivers the dilution method is simulated under unsteady flow conditions. The order of magnitude of most parameters can be found in literature, so that meaningless imaginary rivers can be prevented. In the following, a procedure to obtain these parameter functions is outlined.

3.4.2 System parameter functions

Cross-sectional area

In each position (grid point of the model), the width is supposed to be known. The cross-sectional area is then defined by:

$$A(x,h) = \int_{z_b}^{h} B(x,z)\,\mathrm{d}z \tag{3.81}$$

Velocity distribution parameter α

Two discharge measurements were carried out in the River Grindulu using a current meter. The cross-section was divided in 24 equal and equidistant sections where the flow velocity was measured. On the first day (relatively high discharge) the velocity distibution parameter was $\alpha=1.51$. On the second day (lower discharge) measurements yielded $\alpha=1.56$. The value of α was found by:

$$\alpha = \frac{n^{-1}\sum_{i=1}^{n} u_i^2}{(n^{-1}\sum_{i=1}^{n} u_i)^2} \tag{3.82}$$

which is statistically:

$$\alpha = 1 + (\frac{\sigma_u}{\mu_u})^2 = 1 + r_u^2 \tag{3.83}$$

The role of α in the model is not very significant and estimations between α=1.2 and α=1.8 seem realistic.

fig. 3.17 Measurement of flow velocities using a current meter

Dead zone fraction ß

In the case of a river with groynes the dead zone proportions can be easily estimated. In other cases visual approximations must be carried out. Nordin and Troutman (1980) give values for mountain streams between ß=0.01 and ß=0.06.

Resistance parameter *f*

For steady flows *Q*(*h*)-curves can be found empirically. However, for unsteady flows this relation is not properly defined anymore. An hysteresis effect occurs, which is more significant with increasing time gradients.

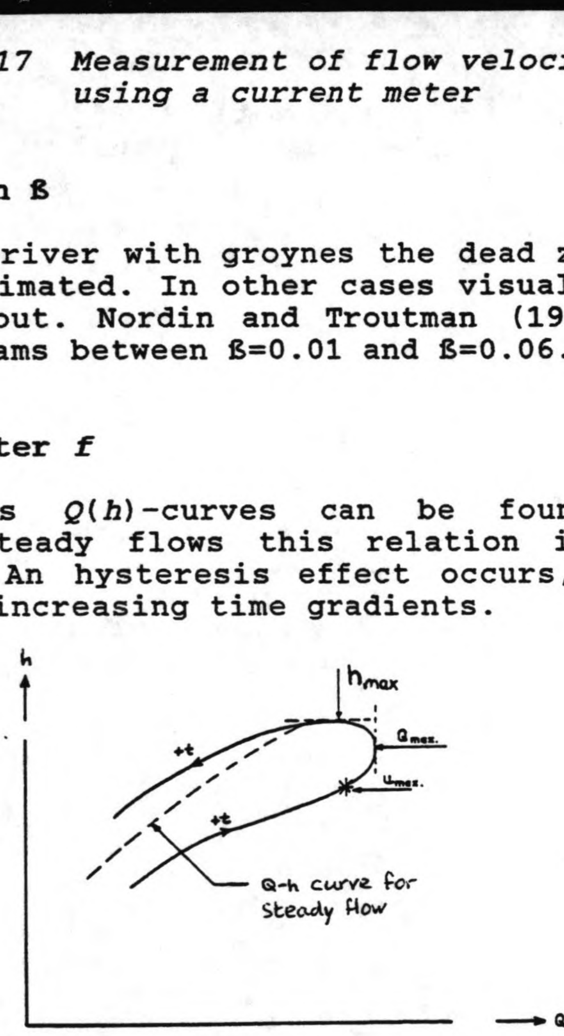

fig. 3.18 Hysteresis in Q(h)-curve

For this reason, both *Q* and *h* are arguments of the resistance parameter *f* (see 3.24).

Its most significant term, the bed friction, can be written as:

$$\frac{P\overline{\tau_b}}{\rho} = \frac{1}{\rho} P(h)\,\overline{\tau_b}(u) \tag{3.84}$$

In (3.84) the influences of h resp. u are separated. The perimeter is geometrically related to the water level. The bottom shear stress is a function of the shear velocities, i.e. a function of the mean flow velocity u. Usually a square proportionality is assumed:

$$\overline{\tau_b} \sim u|u| \tag{3.85}$$

The second term of f, the local pressure deviations due to turbulence, is expressed by:

$$p' = \rho(u')^2 \tag{3.86}$$

The velocity fluctuations u' are linearly related to the mean flow velocity, and so do their gradients. This gives:

$$\frac{\partial}{\partial x}(p'A) \sim u^2 \tag{3.87}$$

If negative discharges are avoided, which is very reasonable for mountain rivers, then both terms are found to be linear with the square of the mean flow velocity. Because $u=Q/A_s$ and $A_s=A_s(h)$, the square of the discharge can be isolated in the expression.
This simplifies f into:

$$f(x,h,Q) = \xi(x,h)\cdot Q^2 \tag{3.88}$$

The cross-sectional geometry is now incorporated in ξ. Substitution of (3.88) into (3.78) under steady flow conditions ($\partial Q/\partial t=0$) yields an expression, in which ξ can be determined by:

$$\xi(x,h) = -\frac{gA_s}{Q_s^2}\frac{\partial h}{\partial x} - \left(\frac{\alpha}{A_s}\right)^2\frac{\partial}{\partial x}\left(\frac{A_s}{\alpha}\right) \tag{3.89}$$

in which the water surface slope $\partial h/\partial x$ is the decisive term.

Q_s is the discharge based on the local steady $Q(h)$ relation. Using a few steady flow profiles, all $\xi(x,h)$ values in the model can be calibrated.

Dispersion coefficient K

A one-dimensional expression for the longitudinal dispersion coefficient (Fischer 1979) is given by:

$$K = \mu \frac{\overline{u}^2 B_s^2}{u_* a} \qquad (3.90)$$

with: $\mu \approx 0.011$
u_* = bed shear-velocity [m/s]

Substitution of the Chézy equation into (3.90) yields:

$$K = \mu \frac{C}{\sqrt{g}} \frac{\overline{u} B_s^2}{a} \qquad (3.91)$$

This expression is only indicative. It shows qualitatively the influence of several geometric parameters. The value μ can deviate with a factor 4.
In the computer model (chapter 4) an overall dispersion coefficient for the river section is required to calibrate μ. Equation (3.91) can then be used for local effects.

Entrainment coefficient D

On the analogy to the dispersion coefficient, an overall value of D is required in the model. Local differentiation is possible.

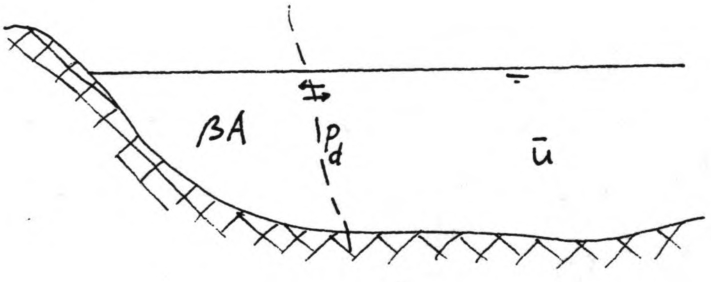

βA = dead zone area [m^2]
P_d = exchange perimeter [m]

fig. 3.19 Exchange of dissolvant between dead zone and flow area

Under the following assumptions of linear relations:

$$D \sim \frac{P_d \overline{u}}{\beta A} \tag{3.92}$$

$$P_d \sim \sqrt{\beta A} \tag{3.93}$$

An expression is found for the entrainment coefficient:

$$D = \omega \frac{\overline{u}}{\sqrt{\beta A}} \tag{3.94}$$

in which ω is a dimensionless coefficient that defines the overall effect of dead zones.

4. Numerical approach

4.1 Simulation of transport processes

Computer models simulating open channel flow and transport processes are available. However, they are usually based on simplified model equations and assumptions of uniformity of shape. The aim of this chapter is the formulation of a computional algorithm, based on the equations (3.82) through (3.85), with all time and place dependent coefficients as specified in section 3.4.2. The effects of a mountain stream with an irregular bed can then be incorporated in the model. These equations are slightly rewritten for the sake of the numerical schemes:

$$\begin{cases} \dfrac{\partial h}{\partial t} + \dfrac{1}{B}\dfrac{\partial Q}{\partial x} = 0 & (4.1) \\[2ex] \dfrac{\partial Q}{\partial t} + \dfrac{\partial}{\partial x}(\alpha \dfrac{Q^2}{A_s}) + gA_s\dfrac{\partial h}{\partial x} + \xi \cdot Q^2 = 0 & (4.2) \\[2ex] \dfrac{\partial \phi}{\partial t} + [u - \dfrac{1}{A_s}\dfrac{\partial}{\partial x}(A_s K)]\dfrac{\partial \phi}{\partial x} - K\dfrac{\partial^2 \phi}{\partial x^2} + \varepsilon D(\phi - \phi_d) = 0 & (4.3) \\[2ex] \dfrac{\partial \phi_d}{\partial t} - D(\phi - \phi_d) = 0 & (4.4) \end{cases}$$

It may be clear that such a model requires a large amount of data and computations. The programming language Matlab proves to be a powerful tool for numerical computations of this kind.

4.2 Explicit and implicit schemes

Different methods exist for the transformation of a differential equation into a numerical algorithm. The choice of the numerical scheme has to be carried out with great care. Criteria like accuracy and stability are of great importance. Numerical schemes can be roughly divided into explicit and implicit schemes. An explicit scheme usually has the form:

$$\mathbf{y}^{n+1} = \mathbf{M}\mathbf{y}^{n} + \mathbf{v}^{n+1} \qquad (4.5)$$

with: $\mathbf{y}^n$ = state vector of time level n

$\mathbf{M}$ = system transition matrix

$\mathbf{v}^{n+1}$ = vector containing boundary conditions

The state vector contains the system variables in the grid points to be calculated (for example river discharges, water levels, concentrations etc.). The state vector of a new time level is a function of the previous time level and the boundary conditions.
An implicit scheme has a slightly different form:

$$M_2 \mathbf{y}^{n+1} = M_1 \mathbf{y}^{n} + \mathbf{v}^{n+1} \tag{4.6}$$

Now the new state vector can only be found after solving a system of linear equations. Although an implicit scheme is more complicated to solve, its advantages are great concerning the stability of the computation. For both the flow equations and the transport equations an implicit difference scheme is chosen. Time derivatives of the state vector are defined in both time levels n and n+1.

4.3 Numerical flow model

4.3.1 Staggered grid or unstaggered grid

In the flow model two system variables are to be integrated: Q and h. Usually a staggered grid is used for the numerical integration of Q and h. This means that the grid points are divided into Q points and h points:

fig. 4.1 Staggered grid in flow model

The grid points at the boundaries should be chosen so that they fit the boundary conditions. The state vector then is:

$$\mathbf{y} = [Q_1 \ h_2 \ Q_3 \ h_4 \ \ldots \ Q_{m-1} \ h_m]^T \tag{4.7}$$

In many cases a staggered grid is very efficient, because the continuity equation contains a time differential in h, and a space differential in Q. The equation of motion contains a time differential in Q, and a space differential in h. The state vectors of different time levels are connected by 'integration molecules':

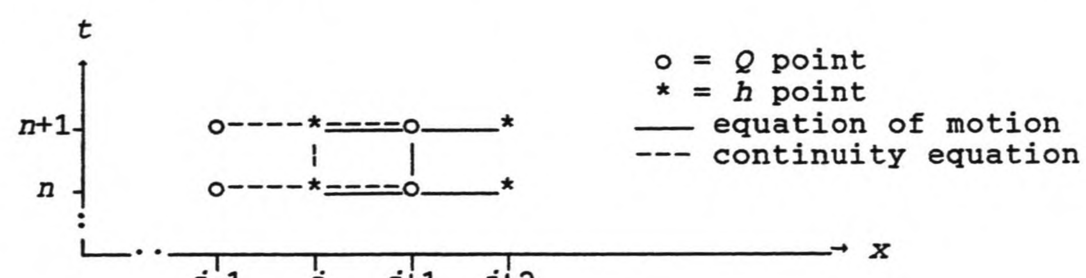

fig. 4.2 Crank-Nicholson integration molecules in a staggered grid

The convective term in the equation of motion does not fit very well in the staggered grid. The expression:

$$\frac{\partial}{\partial x}(\alpha\frac{Q^2}{A_s})$$

needs Q values in h points. This problem can only be solved by accepting an effective grid size of $4\Delta x$ for the convective term.
Another problem connected to the staggered grid is that h dependent parameters (such as A, A_s, B, α, β and ε, see section 3.4.1) can only be defined in h points. But they are necessary in Q points as well. The Q- and h-dependent parameters (such as ξ, u, K and D) cannot be defined at all, because no grid point contains both Q and h. Interpolation could solve this problem, but this would double the effective grid size with negative consequences for accuracy and calculation time.
Moreover, the convection-dispersion model, which cannot be staggered would not fit conveniently to a staggered grid of the flow model.
For these reasons an unstaggered grid is chosen: Q and h are defined in each grid point, and so are all river parameter functions.

fig. 4.3 Unstaggered grid for flow model

In the case of an unstaggered grid, the Preissmann method seems most efficient. Space differentials are defined between two grid points, which makes the effective grid size Δx, instead of Crank-Nicholson's $2\Delta x$. Moreover, modification of the scheme at the boundaries is not necessary.
Now the integration molecules appear as follows:

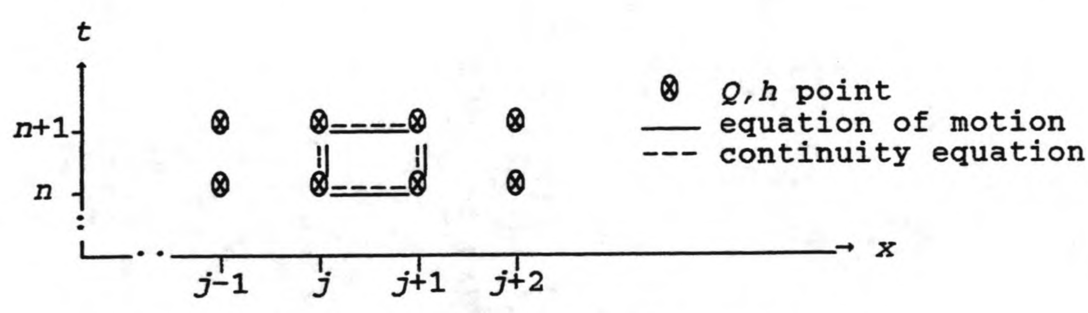

fig. 4.2 Preissmann integration molecule in an unstaggered grid

4.3.2 Discretisation of the differential equations

Preissmann discretisation of the continuity equation (4.1) yields:

$$\frac{1}{2}\left(B_{j-1}\frac{h_{j-1}^{n+1}-h_{j-1}^{n}}{\Delta t}+B_j\frac{h_j^{n+1}-h_j^{n}}{\Delta t}\right)+\Theta\frac{Q_j^{n+1}-Q_{j-1}^{n+1}}{\Delta x}+ \\ +(1-\Theta)\frac{Q_j^{n}-Q_{j-1}^{n}}{\Delta x}=0 \tag{4.8}$$

with: Δt = numerical time step
Δx = numerical spatial step
Θ = time level weighing factor

The spatial differentials represent the centre of the grid interval. Therefore, in order to be central as well, the time differentials in both grid points must be averaged.
The equation of motion (4.2) becomes:

$$\frac{1}{2}\left(\frac{Q_{j-1}^{n+1}-Q_{j-1}^{n}}{\Delta t}+\frac{Q_j^{n+1}-Q_j^{n}}{\Delta t}\right)+\Theta\Bigg\{\frac{[\frac{\alpha Q}{A_s}]_j\,Q_j^{n+1}-[\frac{\alpha Q}{A_s}]_{j-1}\,Q_{j-1}^{n+1}}{\Delta x}+ \\ +\frac{1}{2}g[A_{s,j-1}+A_{s,j}]\frac{h_j^{n+1}-h_{j-1}^{n+1}}{\Delta x}+\frac{1}{2}\left([\xi Q]_{j-1}\,Q_{j-1}^{n+1}+[\xi Q]_j\,Q_j^{n+1}\right)\Bigg\}+ \\ +(1-\Theta)\Bigg\{\frac{[\frac{\alpha Q}{A_s}]_j\,Q_j^{n}-[\frac{\alpha Q}{A_s}]_{j-1}\,Q_{j-1}^{n}}{\Delta x}+\frac{1}{2}g[A_{s,j-1}+A_{s,j}]\frac{h_j^{n}-h_{j-1}^{n}}{\Delta x}+ \\ +\frac{1}{2}\left([\xi Q]_{j-1}\,Q_{j-1}^{n}+[\xi Q]_j\,Q_j^{n}\right)\Bigg\}=0 \tag{4.9}$$

4.3.3 Boundary conditions

If m is the number of grid points, it is easy to see that (4.8) and (4.9) can be implemented in the grid only m-1 times. Two boundary conditions are necessary to make the system consistent. A boundary condition is a Q value, an h value or a $Q(h)$ relation at a boundary. In the case of subcritical flow, each boundary needs a boundary condition. If the flow is supercritical, two upstream boundary conditions are necessary. If transitions of sub- and supercritical flow are present, shock conditions are necessary.

In the flow model of this chapter, subcritical flow is assumed. The downstream boundary condition is given by the formula of Jones, which gives an unsteady $Q(h)$ relation:

$$\frac{\partial h}{\partial t}+ci_s\left\{\left(\frac{Q}{Q_s}\right)^2-1\right\}=0 \tag{4.10}$$

with: c = propagation speed of the flood wave (see 3.54)
Q_s = river discharge based on steady $Q(h)$ relation
i_s = slope of the water surface slope for steady flow ($i_s < 0$)

Another form of this formula is given by (recognise the simple wave structure):

$$\frac{\partial h}{\partial t} + c\frac{\partial h}{\partial x} = ci_s \tag{4.11}$$

In a numerical model (4.11) is more convenient to apply than (4.10). Preissmann discretisation yields:

$$\frac{1}{2}\left(\frac{h_{m-1}^{n+1} - h_{m-1}^{n}}{\Delta t} + \frac{h_{m}^{n+1} - h_{m}^{n}}{\Delta t}\right) + \Theta c\,\frac{h_{m}^{n+1} - h_{m-1}^{n+1}}{\Delta x} + \tag{4.12}$$

$$+ (1-\Theta)\,c\,\frac{h_{m}^{n} - h_{m-1}^{n}}{\Delta x} = ci_s$$

Modification into a supercritical flow model can be made by replacing the subscripts m-1 and m by 1 and 2, respectively.

The upstream boundary condition is the river discharge at x=0:

$$Q_1^{n+1} = Q_1^{n} + \Delta Q^{n+1} \tag{4.13}$$

Figure 4.4 shows the areas of the equations and boundary conditions in the grid.

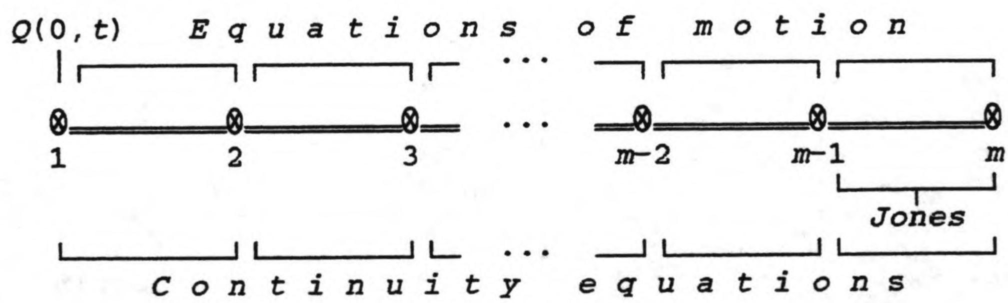

fig. 4.4 Validity areas of model equations

4.3.4 Initial conditions

The initial Q and h values are based on a steady discharge in all sections, equalling the initial upstream boundary:

$$Q_j^1 = Q_1^1 \qquad \text{for } j = 2, \ldots, m \tag{4.14}$$

$$h_j^1 = h_{s,j}(Q_j^1) \qquad \text{for } j = 1, \ldots, m \tag{4.15}$$

in which $h_{s,j}$ is the water level based on the steady $Q(h)$ relation, in grid point j.

4.4 Numerical convection-dispersion model

4.4.1 Discretisation of equations

Equation (4.3) is discretised using the Crank-Nicholson scheme:

$$\begin{aligned}
&\frac{\phi_j^{n+1} - \phi_j^n}{\Delta t} + \Theta\{u_{k,j}\,\frac{\phi_{j+1}^{n+1} - \phi_{j-1}^{n+1}}{2\Delta x} - K_j\,\frac{\phi_{j+1}^{n+1} - 2\phi_j^{n+1} + \phi_{j-1}^{n+1}}{\Delta x^2} + \\
&\qquad + \varepsilon D_j(\phi_j^{n+1} - \phi_{d,j}^{n+1})\} + (1-\Theta)\{u_{k,j}\,\frac{\phi_{j+1}^n - \phi_{j-1}^n}{2\Delta x} + \\
&\qquad - K_j\,\frac{\phi_{j+1}^n - 2\phi_j^n + \phi_{j-1}^n}{\Delta x^2} + \varepsilon D_j(\phi_j^n - \phi_{d,j}^n)\} = 0
\end{aligned} \tag{4.16}$$

in which:

$$u_k = u - \frac{1}{A_s}\frac{\partial}{\partial x}(A_s K) \tag{4.17}$$

discretised as:

$$u_{k,j} = u_j - \frac{1}{A_{s,j}}\,\frac{A_{s,j+1}K_{j+1} - A_{s,j-1}K_{j-1}}{2\Delta x} \tag{4.18}$$

The dead zone differential equation is discretised:

$$\frac{\phi_{d,j}^{n+1} - \phi_{d,j}^n}{\Delta t} - \Theta\, D_j(\phi_j^{n+1} - \phi_{d,j}^{n+1}) - (1- \;)\, D_j(\phi_j^n - \phi_{d,j}^n) \quad 0 \tag{4.19}$$

This equation does not contain any space differential, which enables implementation in each grid point.

4.4.2 Boundaries

At the upstream boundary the concentration in the cross-sectional flow area is a boundary condition:

$$\phi_1^{n+1} = \phi_0 + \frac{M}{Q_1^{n+1}} \tag{4.20}$$

with: ϕ_0 = background concentration of river water [kg/m^3]
M = release of tracer [kg/s]
Q_1^{n+1} = upstream river discharge [m^3/s]

The downstream boundary does not allow a second order derivative, because this requires at least three grid points.

$$\frac{\phi_m^{n+1} - \phi_m^{n}}{\Delta t} + \Theta\{u_{k,m} \frac{\phi_m^{n+1} - \phi_{m-1}^{n+1}}{\Delta x} + D_m(\phi_m^{n+1} - \phi_{d,m}^{n+1})\} + (1-\Theta)\{u_{k,m} \frac{\phi_m^{n} - \phi_{m-1}^{n}}{\Delta x} + D_m(\phi_m^{n} - \phi_{d,m}^{n})\} = 0 \tag{4.21}$$

For this reason the dispersion effect is not taken into account locally and a simple wave scheme is used:

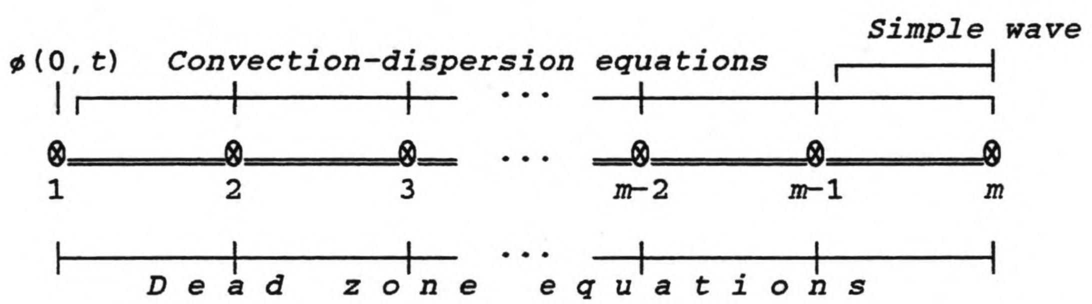

fig. 4.4 Validity areas of model equations

4.4.3 Initial conditions

For general use of the model the initial condition is:

$$\phi_j^1 = \phi_0 \quad \text{and} \quad \phi_{d,j}^1 = \phi_0 \quad \text{for } j=1,\ldots,m \tag{4.22}$$

representing the situation of a natural background concentration in the whole river section.

However, if the effects of unsteady flow on dilution discharge measurements are to be studied, a more efficient initial condition is:

$$\phi_j^1 = \phi_1^1 \quad \text{and} \quad \phi_{d,j}^1 = \phi_1^1 \quad \text{for } j=1,\ldots,m \tag{4.23}$$

This implies an equilibrium state; the release has been taking place continuously for a long time.

4.5 Model performance

4.5.1 Stability

The computation is stable if the norm of the amplification factor (to be defined in 4.25 and 4.29) is less than unity. This is satisfied if:

$$0.5 \le \Theta \le 1 \tag{4.24}$$

for both the Preissmann scheme and the Crank-Nicholson scheme, without any limitations for grid size and time step.
Usually Θ=0.55 is chosen.

4.5.2 Accuracy of the flow model

It is difficult to give a precise prediction about the accuracy of a numerical computation because errors may have several sources. However, a few parameters can be indicative for the accuracy of the result.
For the flow model something can be said about a propagating flood-wave. The numerical flood-wave celerity and the wave damping should not be too deviating from the analytical (true) values.
First a few parameters are defined:

$c = \frac{1}{B}\frac{\partial Q}{\partial h}$ = flood wave celerity

T = period of flood wave

$L = c \cdot T$ = length of flood wave

$\sigma = c\,\frac{\Delta t}{\Delta x}$ = Courant number

$k = 2\pi/L$ = wave number

$\xi = k\Delta x$ = relative grid size

The (complex) amplification factor for the Preissmann scheme is given by (Vreugdenhil 1989):

$$\rho = \frac{1-2(1-\Theta)\,\sigma i \tan(\xi/2)}{1+2\Theta\sigma i \tan(\xi/2)} \tag{4.25}$$

If friction is not taken into account, the numerical flood-wave damping is given by the damping factor d_n:

$$d_n = |\rho|^n \tag{4.26}$$

in which n is the number of time steps. Equation 4.26 shows the accumulating effect of damping in time.

The error in wave-propagation speed is represented by c_r, which is the ratio of the numerical and analytical wave celerity.

$$c_r = -\frac{\arg(\rho)}{2\pi\Delta t/T} \tag{4.27}$$

In an ideal model both values tend tounity. Usually the grid size is not the limiting factor. If ξ is small enough (say $\Delta x/L \leq 1/20$) the time step is decisive for d_n and c_r.

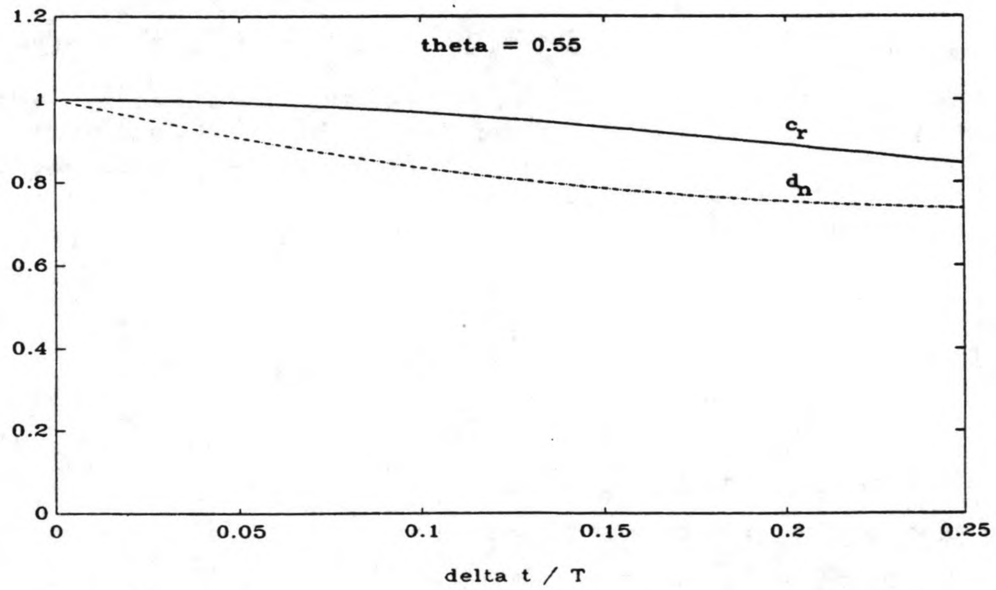

fig. 4.5 Damping factor and relative wave celerity for Preissmann and Crank-Nicholson scheme (after Vreugdenhil 1985)

The numerical damping, caused by friction, can be another source of inaccuracy. The ratio of the numerical and analytical damping due to friction is given by the relative friction damping factor.

$$d_r = \frac{-r\Delta t}{\ln\left(\frac{1-(1-\Theta)r\Delta t}{1+\Theta r\Delta t}\right)} \qquad (4.28)$$

with: r = linearised friction coefficient [s^{-1}]

The value of r is based on a linearisation of the friction term ($f = rQ$). The non-linear relation ($f = \xi Q^2$), could be linearised to:

$r = \xi Q$ with ξ = friction coefficient

Figure 4.6 shows the effect of the term $r\Delta t$ on d_r.

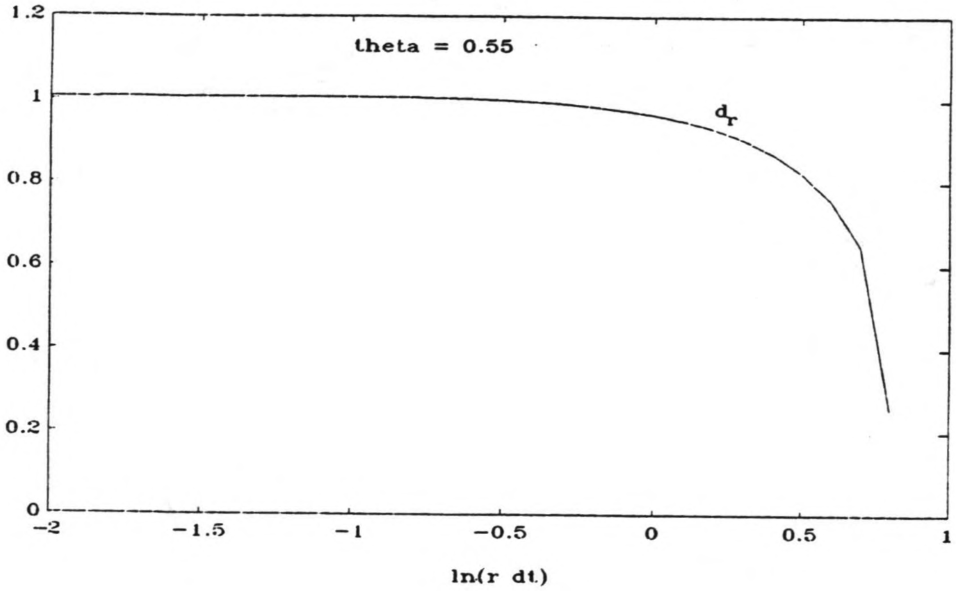

fig. 4.6 Relative friction damping factor (after Vreugdenhil 1985)

4.5.3 Accuracy of the convection-dispersion model

On the analogy of the flood-wave propagation, now a propagating concentration cloud is considered. In order to study the accuracy of a discretised convection-dispersion equation, some of the parameters mentioned earlier, are redefined.

These parameters are:

u = average flow velocity

L = length of cloud

$T = L/u$ = period of cloud

$\sigma = u \frac{\Delta t}{\Delta x}$ = Courant number

$k = 2\pi/L$ = wave number

$\xi = k\Delta x$ = relative grid size

The amplification factor of the Crank-Nicholson scheme is determined by:

$$\rho = \frac{1-(1-\Theta)\sigma i \sin\xi}{1+\Theta\sigma i \sin\xi} \tag{4.29}$$

As already mentioned, for small values of ξ, Crank-Nicholson's amplification factor approaches Preissmann's. Therefore figure 4.5 can be interpreted for the convection-dispersion model as well.
Diffusion in the model can occur even if $K=0$. This is caused by purely numerical effects. The numerical diffusion coefficient for the Crank-Nicholson scheme is (Vreugdenhil 1987):

$$K_{num} = (\Theta-\frac{1}{2})\, u^2 \Delta t \tag{4.30}$$

This value is non-negative for $\Theta \geq 0.5$, in agreement with the stability analysis. The numerical diffusion effect is sufficiently limited for Θ=0.55.

4.5.4 Wiggles

Even if the computation is stable, wiggles can occur. These are oscillating disturbances, usually caused by large concentration gradients. Often, wiggles arise with a sudden change at a boundary (for example a sudden start or stop of a dissolvant release). Such oscillations can be prevented if the cell-Péclet condition is satisfied ($P \leq 2$). The cell-Péclet number is defined by:

$$P = \frac{u\Delta x}{K} \tag{4.31}$$

Although satisfying the cell-Péclet condition is a guarantee that wiggles will not occur, they do not necessarily occur if $P>2$ in the numerical experiments of this study.

Two major reasons can be given for this:

- For a contionuous dissolvant release, concentration gradients will not be high, which makes the system more immune to wiggles.
- The exchange of dissolvant with dead zones has a stabilizing effect on these oscillations.

4.6 The computer programs

The considerations of this and the previous chapter result in a series of computer programs simulating flow and transport processes in a user-defined river section.
These programs, written in Matlab, must be executed from the Matlab environment.
A brief outline of the main principles follows. Figure 4.9 shows the structure of the model and the interaction of the different program files.

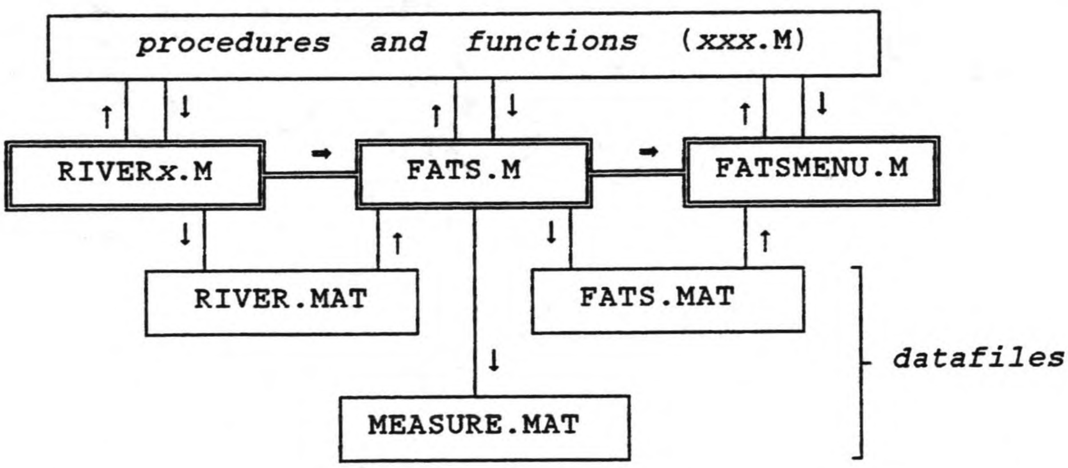

fig. 4.9 Computer files of flow and transport model

First, the RIVER files (RIVER1.M, RIVER2.M, etc.) are user-defined input programs. They contain:

- the definition of the grid (section length, grid size)
- definition of river bed per grid point (by $B(h)$ relations yielding $A(h)$ relations in each grid point)
- definition of flow and dead zone fractions ($\beta(h)$ relations yielding $B_s(h)$ and $A_s(h)$ relations in each grid point)
- definition of the bottom line and a few steady flow profiles (yielding steady $Q(h)$ relations in each grid point and $\xi(h)$ friction functions)
- average values for K and D for one known discharge
- upstream boundary conditions in time: $Q(0,t)$ and $\phi(0,t)$

The program produces plots of the river-section geometry and the boundary conditions, and stores the data in the datafile RIVER.MAT.
The user can add more RIVER files by editing an existing file and changing its name (for example: RIVER4.M).

Secondly, the program FATS.M (flow and transport simulator) contains the time loop and the numerical schemes, by which the numerical integration of Q, h, ϕ and ϕ_d takes place. The results are written in datafile FATS.MAT.

Finally, FATSMENU.M shows the results of the computation. Plots show the effects of wave propagation, convection, dispersion, dead zone effects, hysteresis in unsteady $Q(h)$ curves and the 'measurements' described above.

These sequential programs have a clear *input-compute-output* structure. If a RIVER program is executed, FATS and FATSMENU follow automatically. FATS or FATSMENU can be invoked directly as well. The results, of course, are then based on a previously-generated datafile.

FATS is used to generate dilution discharge measurements in imaginary rivers under unsteady flow conditions. These measurements ($h(0,t)$, $h(L,t)$ and $\phi(L,t)$) are written in datafile MEASURE.MAT. In the next chapter a method is developed to find the original upstream boundary condition $Q(0,t)$ using only these measurements.

5. Determination of the river discharge

5.1 Introduction

In the previous chapter dilution discharge measurements were simulated using the computer model FATS. The upstream river discharge was a boundary condition in this simulation.
The aim of this chapter is to determine this discharge using only the following data:

$$\left.\begin{array}{l} h(0,t) \\ h(L,t) \\ \phi(L,t) \end{array}\right] \text{ 3 continuous measurements}$$

L = length of section [m]
ϕ_0 = background concentration for x<0 [kg/m^3]
$\dot{M}$ = quantity of tracer release [kg/s]

These data can be measured in a real river. In this analysis the data from datafile MEASURE.MAT are used as generated by FATS. No other information is used for the upstream discharge determination.

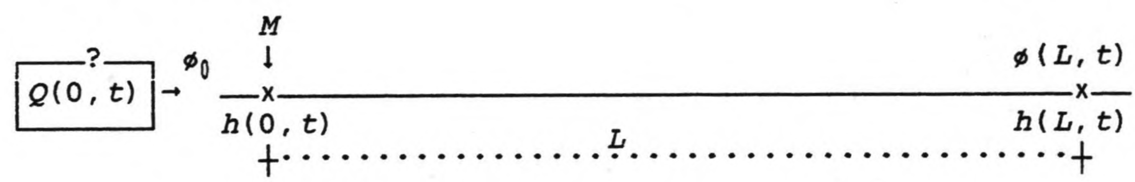

fig. 5.1 Discharge dilution method under unsteady flow conditions

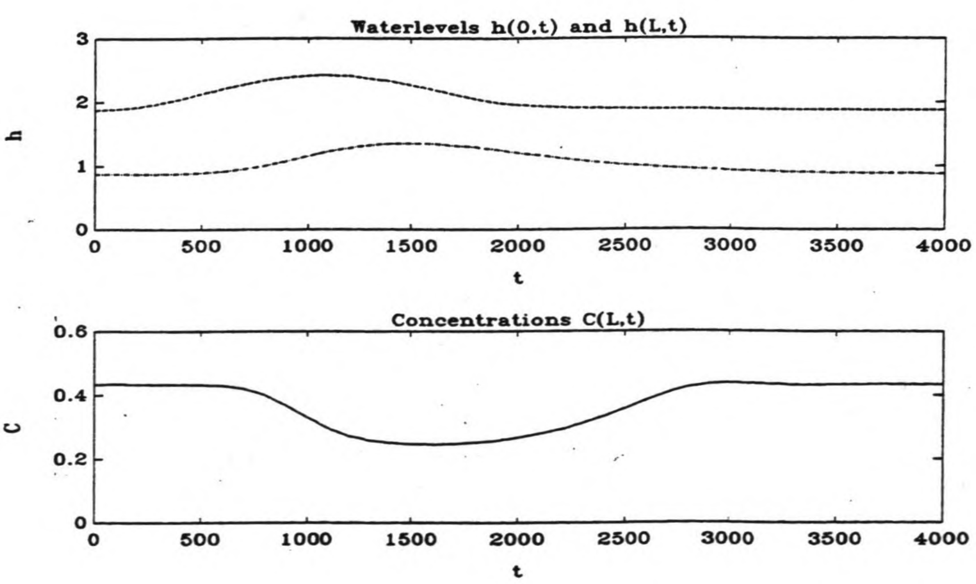

fig. 5.2 Measurements of $h(0,t)$, $h(L,t)$ and $\phi(L,t)$, generated by FATS

5.2 Reconstruction of the flood wave

5.2.1 Introduction

A dynamic reconstruction model is required to determine $Q(0,t)$. A first estimation of the river discharge is given by the steady state formula (see 2.14, or Noppeney 1987):

$$Q_m(t) = \frac{M}{\phi(L,t) - \phi_0} \tag{5.1}$$

Q_m is considered a 'measured' discharge replacing the measured downstream concentration. Q_m contains a phase shift with regard to the unknown $Q(0,t)$, caused by the transportation time from $x=0$ to $x=L$. Besides, its shape is distorted by dispersion, unsteady velocities, dead zones, etc.

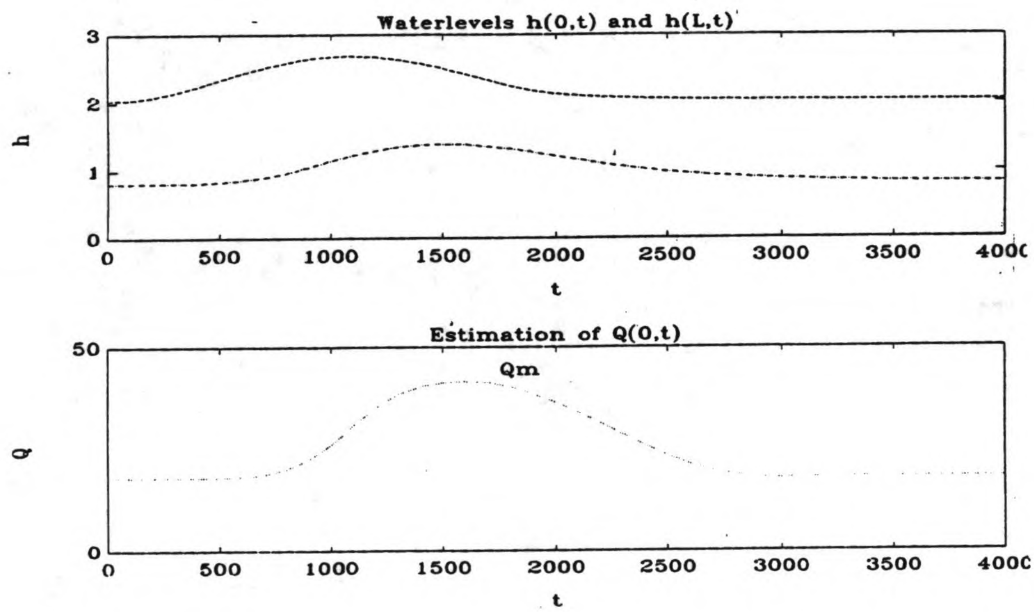

fig. 5.3 'Measured' discharge Q_m

5.2.2 Parameter estimation

In order to reconstruct the flood wave, river parameters such as widths, bottom levels, roughness, etc. are required. It is impossible to find all original time and place-dependent coefficients as pointed out in section 3.4.2, because the three measurements do not contain all this information.
It is sufficient to find a computational geometry and an upstream discharge yielding observations equal to the measurements. This section discusses a procedure to estimate the parameters of such a geometry.

Consider a geometry in which nearly all parameters are constant. Each cross-section is rectangular; the coefficients ß, C, i_b, µ are constant. The convective term in the equation

<u>System parameters:</u>

z_0 z_L B_0 B_L ß C µ D

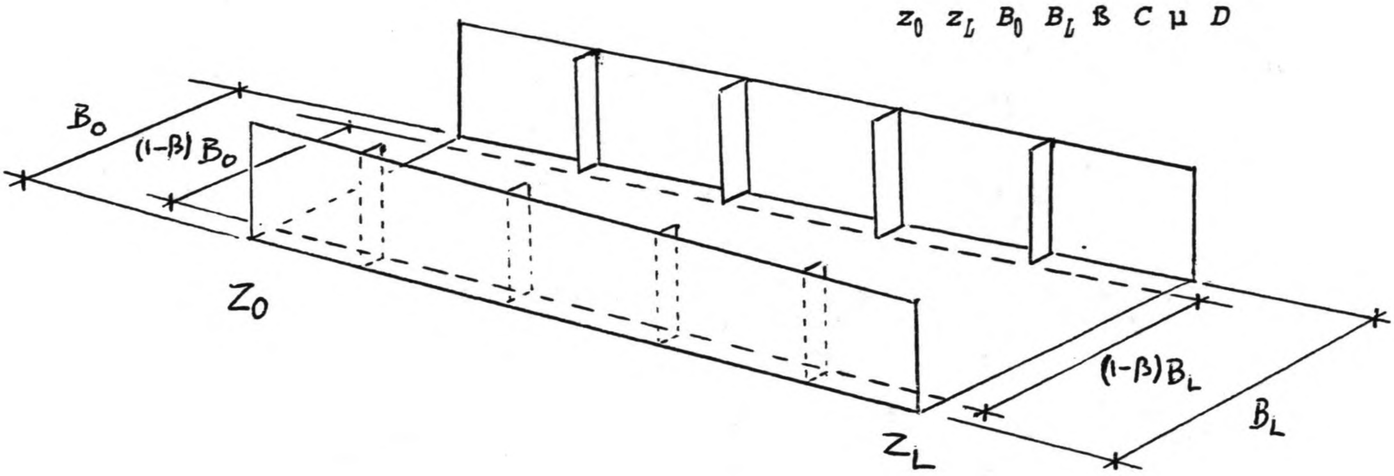

fig. 5.4 Computational geometry for flood wave reconstruction

of motion uses α=1. The width can deviate as a linear function of x. This enables a manipulation of the flood wave damping on top of the friction effect.
In order to estimate the parameters, flow formulas (Chézy, Jones) are used. Although theoretically not entirely correct, the following expressions yield a reasonable first-order approximation:

$$Q_{min} = \min(Q_M) \tag{5.2}$$

$$Q_{max} = \max(Q_M) \tag{5.3}$$

$$i_b = \frac{h_{0,min} - h_{L,min}}{L} \tag{5.4}$$

$$c = \frac{L}{t(h_{L,max}) - t(h_{0,max})} \tag{5.5}$$

$$\overline{u} = \frac{L}{t(Q_{M,max}) - t(h_{0,max})} \tag{5.6}$$

The celerity c and velocity $\overline{u}$ have a geometrical relation:

$$c = \frac{3}{2}(1-ß)\,\overline{u} \tag{5.7}$$

yielding an expression for the dead-zone coefficient:

$$\beta = 1 - \frac{2c}{3\overline{u}} \tag{5.8}$$

For the lowest water level in x=0 the steady flow equation (Chézy) is formulated as:

$$Q_{min} = (1-\beta)\, B_0\, C(h_{0,min} - z_0)^{3/2}\, i_b^{1/2} \tag{5.9}$$

with unknown B_0, C and z_0. For the highest water level the flow equation requires an unsteady extension (Jones):

$$Q_{max} = \max\{ (1-\beta)\, B_0\, C[h(0,t) - z_0]^{3/2}\, i_b^{1/2} \sqrt{1 + \frac{\partial h/\partial t}{c i_b}} \} \tag{5.10}$$

A third equation, describing the average flow velocity during the passage of the top of the flood wave, makes B_0, C and z_0 defined:

$$\overline{u} = C\sqrt{i_b\,(h_{0,max} - z_0)} \tag{5.11}$$

The other parameters are (initially) defined by the following assumptions:

$$B_L = B_0 \tag{5.12}$$

$$z_L = z_0 - L i_b \tag{5.13}$$

$$\mu = 0.011 \tag{5.14}$$

$$D = 0 \tag{5.15}$$

5.2.3 Reconstruction model

The differential equations used for the reconstruction model are the same as described in section 4.1 (equations 4.1 through 4.4). The flow equations are again discretised by the Preissmann scheme, and the transport equations by the Crank-Nicholson scheme.

The measured water level $h(0,t)$ is an upstream boundary condition in the flow model. As a downstream boundary condition $h(L,t)$ can be taken, or the Jones formula. Using the

Jones formula has the great advantage that a new observation of $h(L,t)$ is generated, which is not necessarily equal to the measurement. Actually, their alikeness indicates the quality of the reconstruction.
The flow model directly produces a $Q(0,t)$, which is immediately used in the upstream boundary condition of the transport model:

$$\phi(0,t) = \phi_0 + \frac{M}{Q(0,t)} \tag{5.16}$$

The transport model produces a downstream observation of the concentration, which is directly translated into a $Q_{\mathbf{m}}$ measurement. Comparison with the original $Q_{\mathbf{m}}$ curve gives a second impression of the quality of the flood-wave reconstruction.

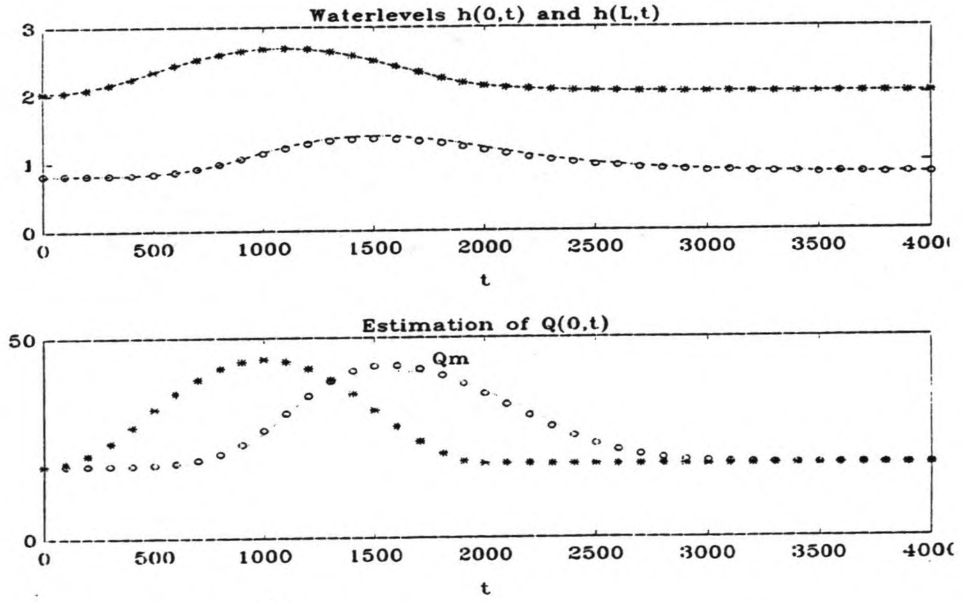

fig 5.5 Reconstruction of the flood wave, plotted with the measurements (first approximation)

Figure 5.6 shows the sequential procedures, each symbolised by a letter (*H*, *S*, *F*, *H*). Vector X is the real world (water levels, discharges, concentrations in time and space), in which measurements Y were found. Based on Y the river geometry parameters Θ are estimated and used in the flood wave reconstruction. X' is the world inside the model (computed water levels, discharges, concentration in time and space grid) containing $Q(0,t)$. A new observation Y' (i.e. $h(L,t)$ and $\phi(L,t) \rightarrow Q_{\mathbf{m}}$, see fig. 5.5) is an indicator of the confidence one can have in the reconstruction, and thus in $Q(0,t)$ (plotted as *, fig. 5.5).

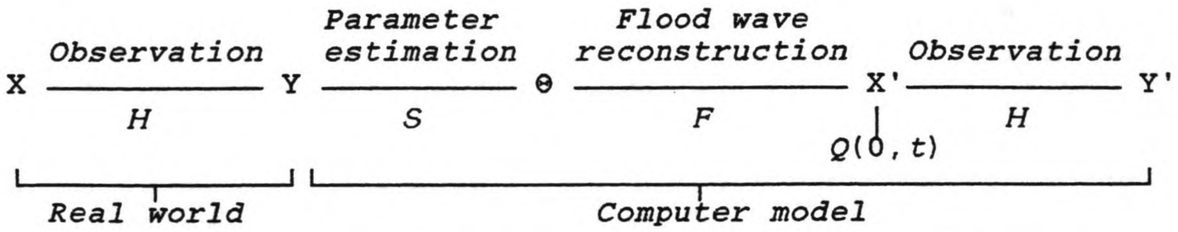

fig. 5.6 Schematisation of reconstruction procedure

If Y' differs from Y, the error could have been introduced in each part of the chain. The measurement errors in *H*, caused by inaccuracy of the equipment, should be limited, but are beyond control of the model. The numerical errors which occur in the reconstruction *F* can be controlled within reason. For this reference is made to section 4.5. The greatest error is introduced in the parameter estimation *S*. If the river parameters Θ can be improved so that Y'=Y, the model and $Q(0,t)$ as determined can be trusted.

5.3 Parameter identification problems

5.3.1 Introduction

The determination of the parameters in a system is an identification problem. Various theories exist to solve identification problems. For a general consideration, the following variables are defined:

Θ = parameter vector, to be identified

p = number of elements in Θ

f(Θ) = operator, using Θ, producing a new observation (see fig. 5.6 : f(Θ) = *HF* Θ = Y')

Y = true observation vector

n = number of elements in Y and f

$J(\Theta) = \| Y - f(\Theta) \|^2$ = cost function to be minimised

The model observation Y' is considered to be a function of the parameter vector Θ: Y'=f(Θ) in the spaces ($R_p \rightarrow R_n$). The alikeness of Y and f(Θ) is a criterium for the quality of the parameters, expressed by the cost function J(Θ).

5.3.2 Procedures using derivatives

Usual methods investigate the influence of each parameter on each observation (i.e. the influence of each Θ element on each Y element). The heart of such an improvement procedure is the derivative $\partial Y/\partial\Theta$. This is a Jacobian matrix of the form:

$$\frac{\partial Y}{\partial \Theta} = \begin{bmatrix} \frac{\partial Y1}{\partial \Theta 1} & \cdots\cdots & \frac{\partial Y1}{\partial \Theta p} \\ \vdots & & \vdots \\ \frac{\partial Yn}{\partial \Theta 1} & \cdots\cdots & \frac{\partial Yn}{\partial \Theta p} \end{bmatrix} \qquad (5.17)$$

This matrix ensures an optimal first-order parameter improvement. The determination of this matrix is a significant time and memory consuming operation. For one iteration, p function evaluations are required. In the identification problem of this study a function evaluation means a complete time loop of the flood-wave reconstruction.

5.3.3 DUD (doesn't use derivatives)

An attractive alternative for parameter identification problems is presented by DUD (Ralston and Jennrich 1978). DUD is a derivative free algorithm, that gives a parameter improvement iteration for each function evaluation (instead of p evaluations).

Experiences show that up to ten constant (lumped) parameters can be identified quite efficiently using DUD. For larger numbers of parameters convergence problems or even robustness problems may occur. In the identification problem of this study eight parameters are to be identified (see fig. 5.4), and DUD is a useful tool.

The variables in the identification problem of this study, are defined by:

$$\Theta = [\ z_0 \quad z_L \quad B_0 \quad B_L \quad C \quad ß \quad \mu \quad D\ ]^T \qquad (5.18)$$

$$p = 8 \qquad (5.19)$$

$$f(\Theta) = [\ h(L,0) \ \ .. \ \ h(L,T) \quad \phi(L,0) \ \ .. \ \ \phi(L,T)\ ]^T \qquad (5.20)$$

generated by reconstruction model

$$Y = [\ h(L,0) \ \ .. \ \ h(L,T) \quad \phi(L,0) \ \ .. \ \ \phi(L,T)\ ]^T \qquad (5.21)$$

from datafile MEASURE.MAT

$$n = 2\,(T/\Delta t + 1) = 2 \times \text{number of time steps} \tag{5.22}$$

$$J(\Theta) = \sum_{i=1}^{n} [Y_i - f_i(\Theta)]^2 \tag{5.23}$$

DUD needs $p+1$ function evaluations, generated using different parameter vectors (non-singular, stretching a p-dimensional space), before a new Θ can be created. These vectors must be numbered (suffix k, $k=1,..,p+1$) so that:

$$J(\Theta_1) \geq .. \geq J(\Theta_k) \geq .. \geq J(\Theta_{p+1}) \tag{5.24}$$

implying that iteration $p+1$ was the best. The parameter vectors and their evaluations are stored in the matrices:

$$\Delta\boldsymbol{\Theta} = \begin{bmatrix} \vdots & & \vdots & & \vdots \\ \Theta_1-\Theta_{p+1} & .. & \Theta_k-\Theta_{p+1} & .. & \Theta_p-\Theta_{p+1} \\ \vdots & & \vdots & & \vdots \end{bmatrix} \tag{5.25}$$

$$\Delta F = \begin{bmatrix} \vdots & & \vdots & & \vdots \\ f(\Theta_1)-f(\Theta_{p+1}) & .. & f(\Theta_k)-f(\Theta_{p+1}) & .. & f(\Theta_p)-f(\Theta_{p+1}) \\ \vdots & & \vdots & & \vdots \end{bmatrix} \tag{5.26}$$

The sizes of these matrices are $p\times p$ and $n\times p$, respectively.

DUD's linear approximation of a new parameter vector is written as a function of α (α is a vector in p-dimensional Θ space):

$$\Theta_{new} = \Theta_{p+1} + \Delta\boldsymbol{\Theta}\,\alpha \tag{5.27}$$

The linear approximation ℓ of f is given by:

$$\ell(\alpha) = f(\Theta_{p+1}) + \Delta F\,\alpha \tag{5.28}$$

The residue of the linearisation is to be minimised:

$$J_{\ell(\alpha)} = \| Y - \ell(\alpha) \|^2 \tag{5.29}$$

Its solution is given by:

$$\alpha = (\Delta F'\Delta F)^{-1}\Delta F'(Y-f(\Theta_{p+1})) \tag{5.30}$$

The algorithm can be described by:

1. Assume $p+1$ Θ vectors as in (5.18)
2. Generate the corresponding $f(\Theta)$ observations (5.20)
3. Compute their cost functions $J(\Theta)$ by (5.23)
4. Define $\Delta\boldsymbol{\Theta}$ and ΔF by (5.25) and (5.26), satisfying (5.24)
5. Find the α vector from the linear system (5.30)
6. Find the new Θ vector by (5.27)

Repeated iteration

The new parameter vector can be used for a second iteration. After another function evaluation using Θ_{new}, $p+2$ Θ vectors and $f(\Theta)$ vectors are available. The vectors with the highest cost function (Θ_1 and $f(\Theta_1)$) can be deleted, and the others are renumbered satisfying (5.24). This extends the algorithm to:

7. Execute the function evaluation $f(\Theta_{new})$
8. Compute its cost function by (5.23)
9. Erase Θ_1 and $f(\Theta_1)$, and renumber the remaining vectors from 1 to $p+1$ satisfying (5.24)
10. Return to step 4

This process can be repeated until no significant decrease of the cost function occurs anymore.
The Θ vector with the lowest $J(\Theta)$ represents the river geometry that can be trusted most. The $Q(0,\cdot t)$ hereby generated is the result of the computation.

5.4 The computer programs

The procedures necessary for the discharge determination are executed by two sequential computer programs (fig. 5.7).

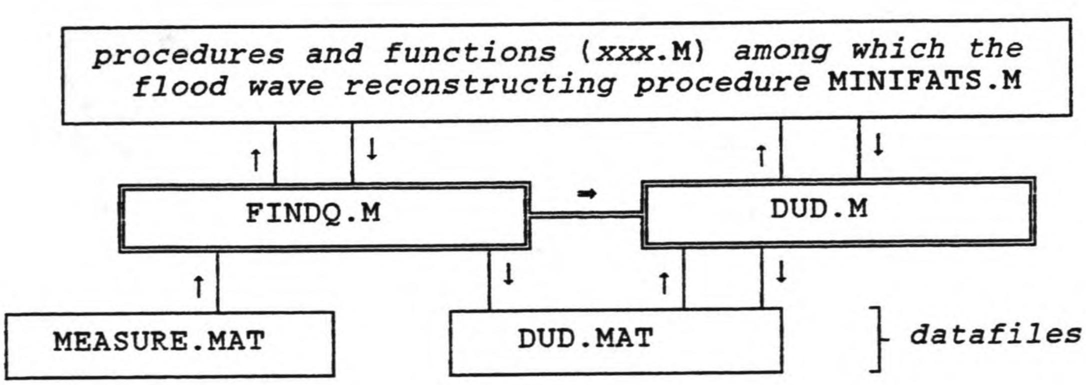

fig. 5.7 Computer files for discharge determination

First, the program FINDQ.M reads the measurements from datafile MEASURE.MAT and makes a first parameter estimation as described in section 5.2.2. The program reconstructs the flood wave as described in section 5.2.3 using the external procedure MINIFATS. Eight more such iterations take place (total nine iterations, $p=8$), in which FINDQ slightly modifies the elements in the Θ vector. The nine Θ vectors and their corresponding $f(\Theta)$ vectors and $J(\Theta)$ values are written in datafile DUD.MAT. Actually, FINDQ executes steps 1, 2 and 3 of the algorithm described in the previous section. After this, the user is asked to start the DUD parameter identification.

Once the datafile DUD.MAT exists, DUD can be invoked directly without FINDQ. The program executes steps 4 to 10 as described in section 5.3.3. After each iteration the datafile DUD.MAT is updated, and the user is asked permission for a next iteration. This enables the parameter improvement to take place during different sessions. This makes DUD a learning and non-forgetting computer program. DUD quits the loop if the cost function is no longer decreasing.
Both FINDQ and DUD store the most reliable upstream discharge $Q(0,t)$ found thus far (i.e. with the lowest cost function) in vector Q_{best} in datafile DUD.MAT, and inform the user continuously about the identified parameters and cost functions.

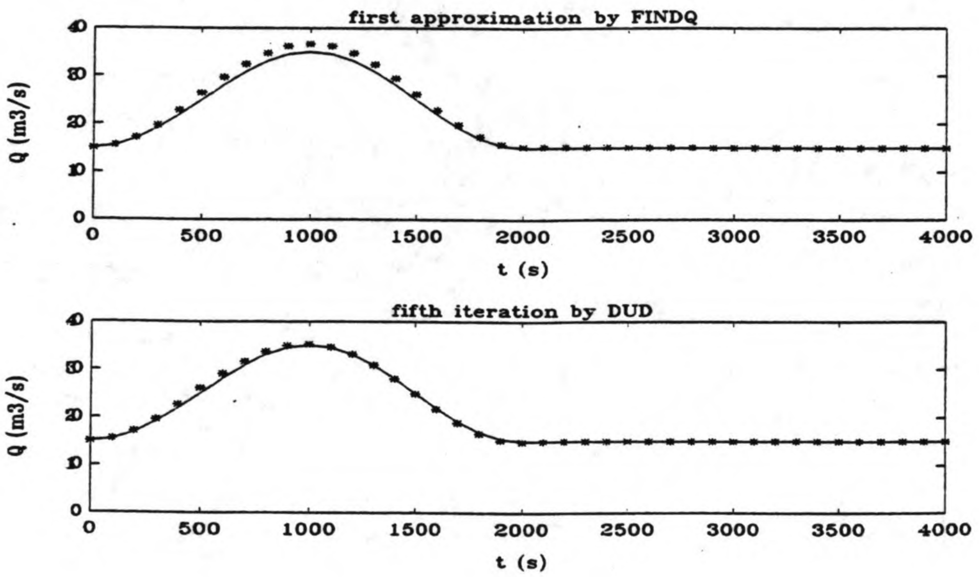

fig. 5.8 Flood wave reconstruction (determined, — true)*
Upper graph: first approximation by FINDQ
Lower graph: fifth DUD-iteration

5.5 Experiments

5.5.1 Introduction

The plots in this chapter are results of an experiment using the computer programs RIVER, FATS, FINDQ and DUD.
The data are arbitrarily chosen:

$L = 1000$ m	river section length
$i_b = 10^{-3}$	average bottom slope
$B \approx 10$ to 20 m	width (water level dependent)
$\beta = 0.01$	dead zone fraction
$K \approx 12$ m^2/s	dispersion coefficient (flow dependent)
$D \approx 0.02$ s^{-1}	entrainment coefficient (flow dependent)
$Q_{min} = 15$ m^3/s	minimum discharge
$Q_{max} = 35$ m^3/s	maximum discharge
$T_w = 2000$ s	flood-wave period
$T = 4000$ s	computation period
$\phi_0 = 0.1$ kg/m^3	background concentration
$M = 5$ kg/s	tracer release
$\Delta x = 100$ m	spatial step } in numerical grid
$\Delta t = 300$ s	time step } in numerical grid

The discharge is a cosine function remaining steady after one period. The programs FINDQ and DUD determine this discharge using the data mentioned in section 5.1. As the figures show, the iterations converge towards the right solution (fig. 5.8).

5.5.2 Measurement noise

The use of a measured water level as an upstream boundary condition is questionable.
Since the river discharge is usually more than linearly related to the water level, measurement noise will be amplified in the river discharge. This causes propagating short waves resulting in numerical wiggles (fig. 5.9).
In this experiment deviations were introduced:

$$\sigma_h = 0.02 \text{ m} \tag{5.25}$$

$$r_\phi = 0.02 \tag{5.26}$$

$$r_M = 0.02 \tag{5.27}$$

Deviations in water level measurements are usually of an absolute magnitude. Measurements of concentration and tracer release usually contain deviations of a relative magnitude. This is related to the measurement device (chapter 6).

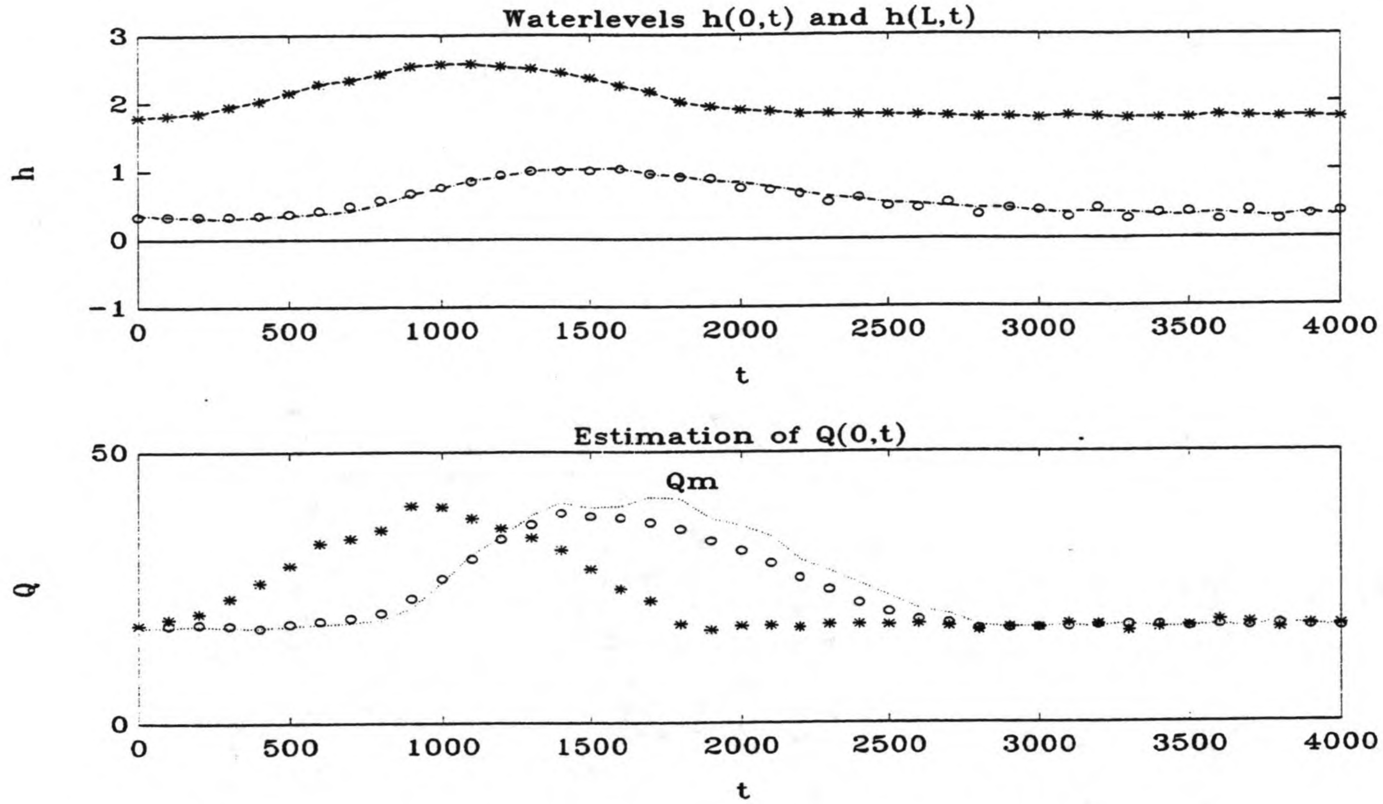

fig. 5.9 Flood wave reconstruction using noisy measurements

The wiggles, caused by noise in $h(0,t)$, become dominant in the cost function. This makes the filtering procedure lose its effectivity. However, noise in the other two measurements $h(L,t)$ and $\phi(L,t)$ hardly seem to effect the procedure because they are not used actively. Instead, they are used passively as observations. A fundamental question about the implementation of identification procedures arises.

Theoretically an observation should not be used as a boundary condition in an identification procedure. However, a boundary condition is required and another one is not available. A solution to this problem could be the use of an hypothetical upstream river discharge as a boundary condition. The measured upstream water level can then be used as an observation.
This discharge then is an object to be identified too, containing as many elements as there are time steps in the computation. This means that $p=(T/\Delta t+1)+8$. In the case of this simple example, it would mean that $p=49$ instead of $p=8$ (5.19). As explained in section 5.3.2, DUD should not be chosen for an identification problem of this magnitude. Algorithms, using derivatives, are required needing 49 function evaluations per iteration instead of one. On a 12 MHz personal computer each iteration step would then take more than 3 hours instead of 4 minutes. A better result is not even ensured.
This is not a recommendable way to avoid problems with measurement noise.

In practice measurement noise can be smoothed by increasing the observation frequency (i.e. reducing the observation interval). If, for example, the observation interval is a fifth of the numerical time step, the noise is already significantly reduced (fig. 5.10). This effect can be sufficient to avoid the wiggles.

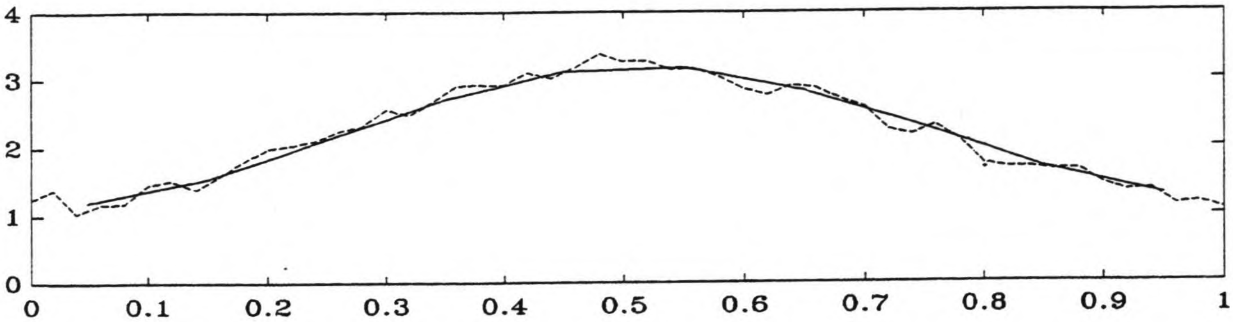

fig. 5.10 Smoothing effect of observation averaging

The device for the water level measurement recommended in the next chapter, produces a noise ($\sigma_h \approx 3.5$ mm) much lower than in this example. Additionally, the observation interval of automatic registration can be adjusted down to 0.4 s. This implies that measurement noise effects can be entirely liquidated.
Steady deviations, however (especially for concentration and spill measurements), have more serious consequences for the result. These can only be avoided by regular calibration of the equipment.

5.3.3 TRISULA

Until now the flood wave reconstruction procedure MINIFATS uses measurements generated by FATS. Both simulation models are based on the same numerical schemes and use the same space and time grid.
As a test for the robustness of the FINDQ-DUD system measurements are generated using the computer model TRISULA (Delft Hydraulics). This program simulates a dilution test under unsteady flow conditions using unknown numerical schemes and an unknown grid in an unknown river geometry.

The known data are:

L = 10 km	river section length
ϕ_0 = 0 kg/m^3	backgound concentration
M = 1 kg/s	tracer release

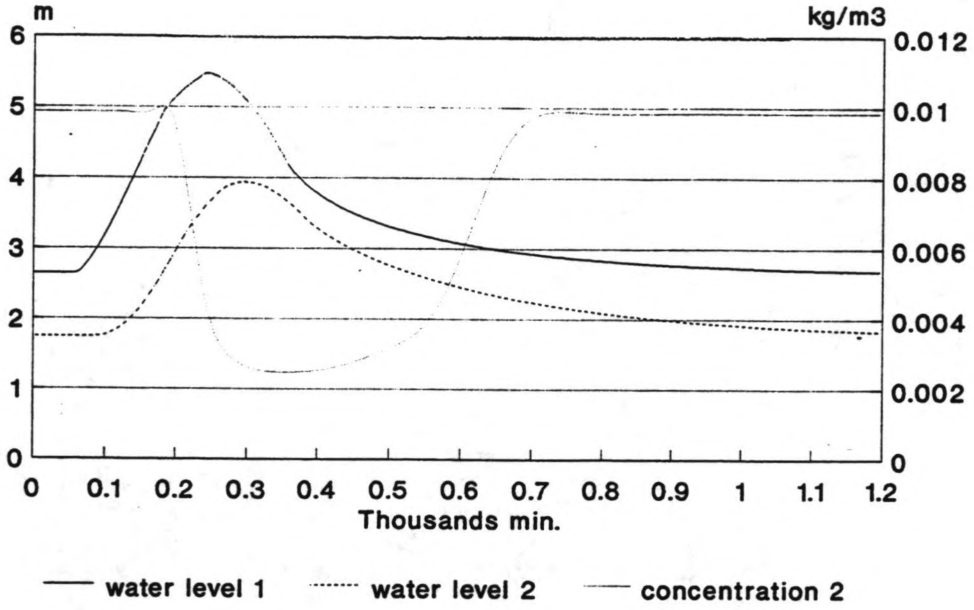

fig. 5.11 Measurements generated by TRISULA

After eleven DUD iterations, the cost function ceases to decrease. The discharge then determined is shown in figure 5.12. Figure 5.13 shows the river discharge, used in the TRISULA model. In figure 5.14 both are plotted.
Although unsteady effects in both flow models appear to be somewhat different, this experiment proves the robustness and convergence qualities of the FINDQ-DUD algorithm.

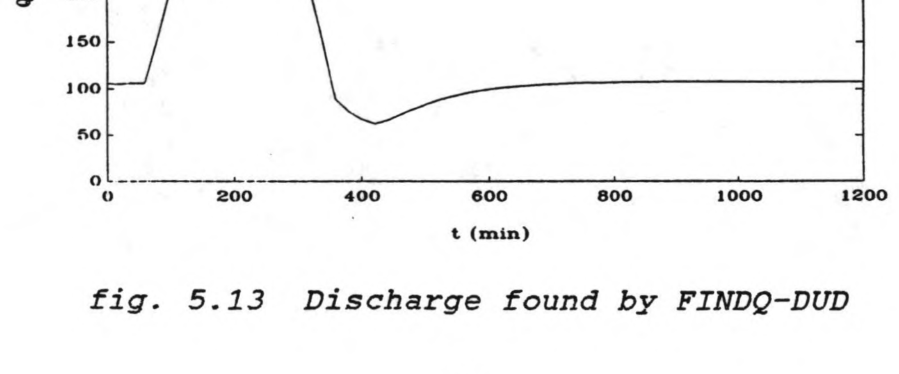

fig. 5.13 Discharge found by FINDQ-DUD

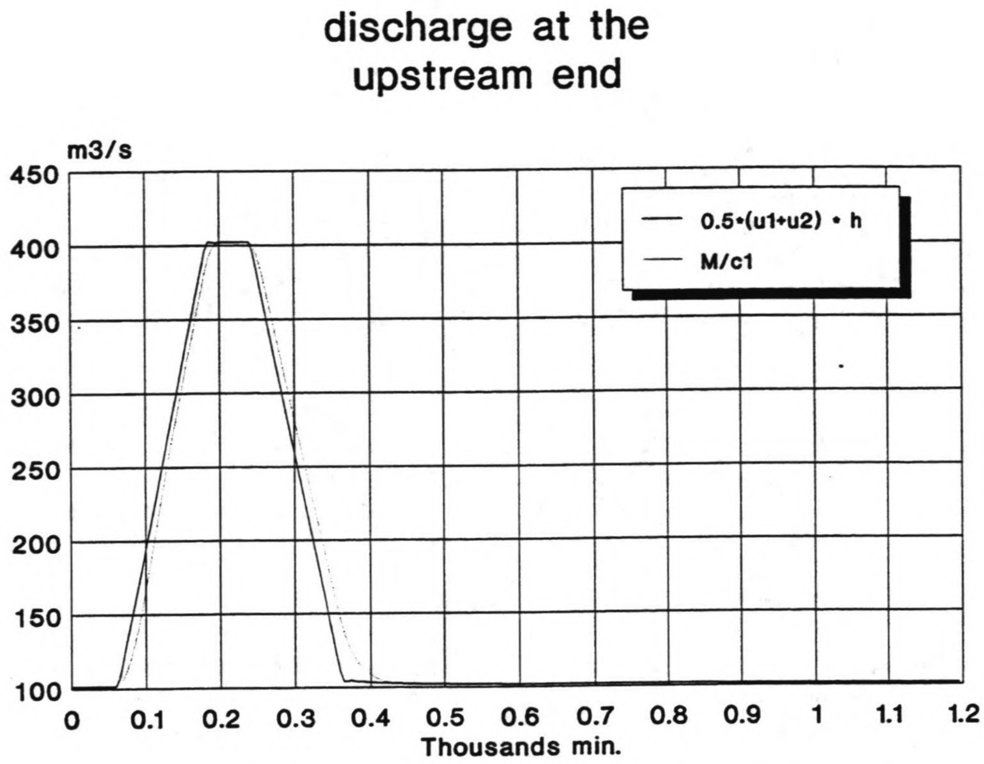

fig. 5.12 Discharge used by TRISULA

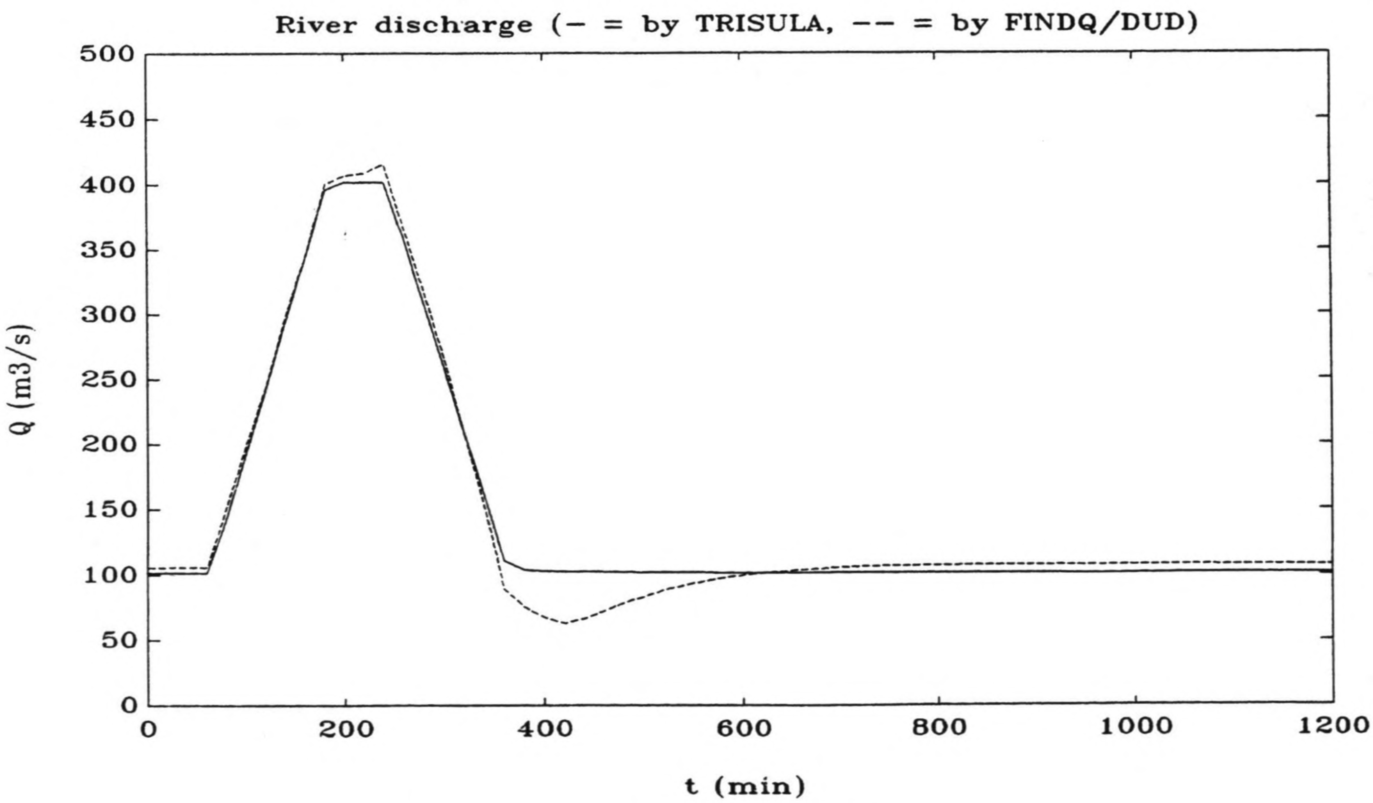

fig. 5.14 Both discharges plotted in one figure

6. Field work device

6.1 Introduction

The computational algorithm for the determination of an unsteady river discharge needs measurements that thus far have been provided by FATS and TRISULA. The results can be compared to the original upstream boundary condition (fig. 5.8, fig. 5.14).

Since the DUD iterations prove to converge towards the right solution, the algorithm seems able to deal with real measurements. This chapter discusses the methods and the device to obtain the required measurements in a natural stream.

6.2 The measurement network

A possible design of the measurement network consists of the following elements:

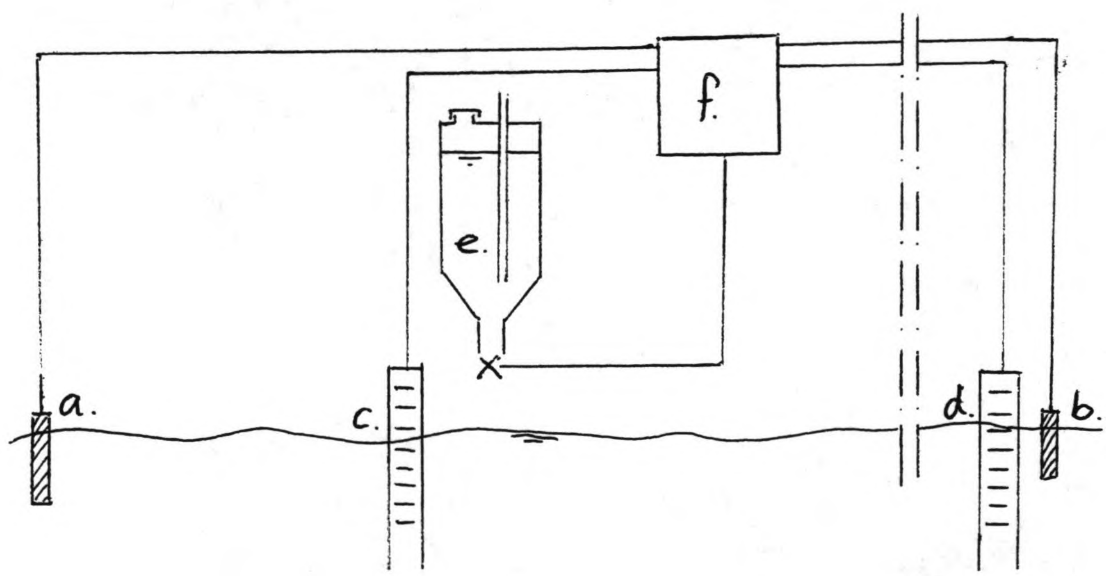

fig. 6.1 Network of measurement and control device

a. Conductance meter (at $x<0$) for the background concentration measurement
b. Conductance meter (at $x=L$) for diluted tracer measurement
c. Water level measurement at $x=0$
d. Idem at $x=L$
e. Tracer-releasing device (i.e. vessel, or tank) with valve
f. Datalogger, digital datarecorder and programmable controller

6.3 The device

6.3.1 Conductance meter

Conductance meters connected to conductivity cells are used for the concentration measurements (see also: chapter 2).

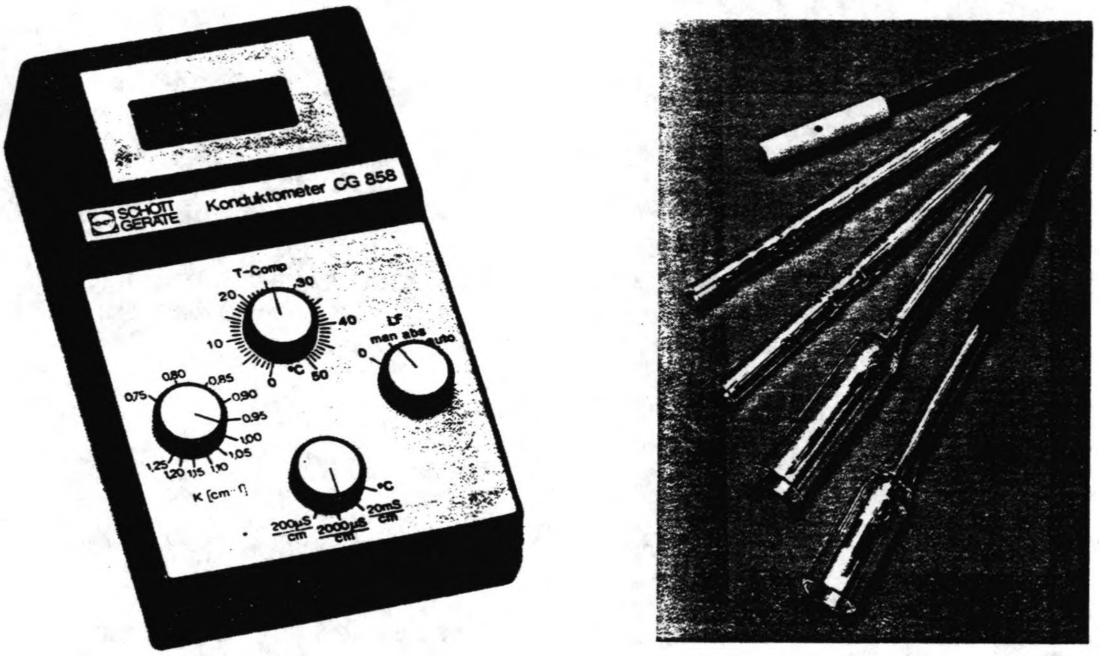

fig. 6.2 Conductance meter and cells with different cell constants

The cell contains two platinum plates with an adjusted distance enabling an electric current to pass through the conductant fluid. The electric current indicates the conductance of the fluid.

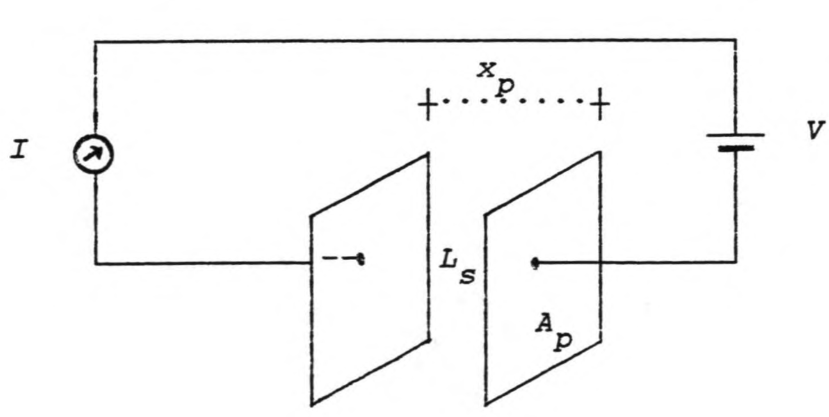

fig. 6.3 Conductance (L_s) of a medium

The electric conductance is expressed by:

$$L_s = \frac{K}{R} = \frac{KI}{V} \tag{6.1}$$

with: V = voltage over electrodes [V]
I = electric current through medium [A]
R = electric resistance of the medium [Ω]
K = cell constant (i.e. plate distance per unit of surface area x_p/A_p, usually in cm^{-1})

The conductance, usually expressed in μS/cm (S=Siemens=Ω^{-1}), is very temperature dependent. Therefore, if the concentration is to be determined from the electric conductivity, the temperature effect should be compensated. Usually a specific conductance is defined, representing the fluid conductance for T=25°C. An empiric relation between the specific conductance and concentration of a NaCl solution is given by:

$$\phi = 3.24 \cdot 10^{-4} \; L_s^{1.058} \tag{6.2}$$

with: L_s = specific conductance for T=25°C (μS/cm)
ϕ = NaCl concentration (‰ i.e. kg/m^3)

This (nearly) linear relation is obtained by a least-square-fitting in a logarithmic graph, where experimentally found $\phi(L_s)$ couples were plotted.

Often, conductance meters are able to compensate for the temperature effect automatically. The cell contains a temperature sensor and the conductance meter interprets the electric conductance and the temperature, and converts them directly into the specific conductance.

If a datalogger is used, the cells can be connected directly to it without the use of the conductance meter. Both the temperature and the electric conductance must be registered on the memory card. The tracer concentration can then be determined.

6.3.2 Measurement of water levels

The simplest device for water level measurement is the staff gauge.

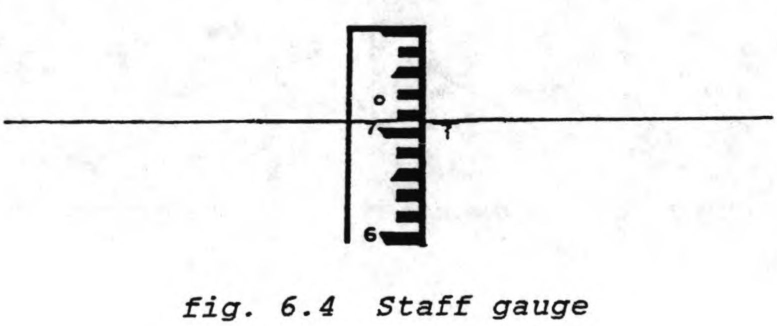

fig. 6.4 Staff gauge

The staff gauge is a directly-readable but not very accurate gauge. Wave fluctuations make the observation inaccurate and connection to a data-recording device is impossible.

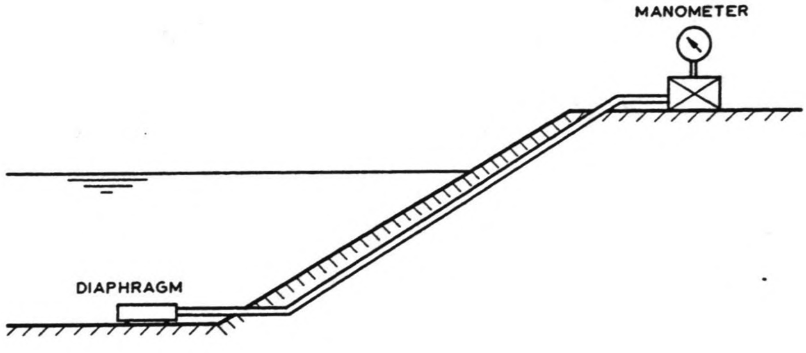

fig. 6.5 Diaphragm-type pneumatic gauge

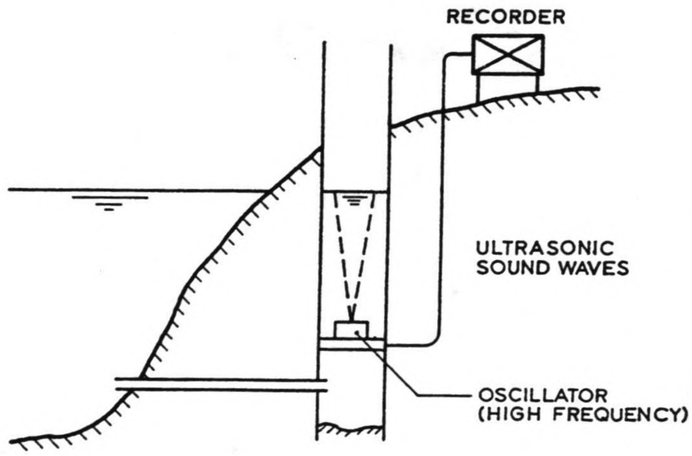

fig. 6.6 Electro-magnetic gauge

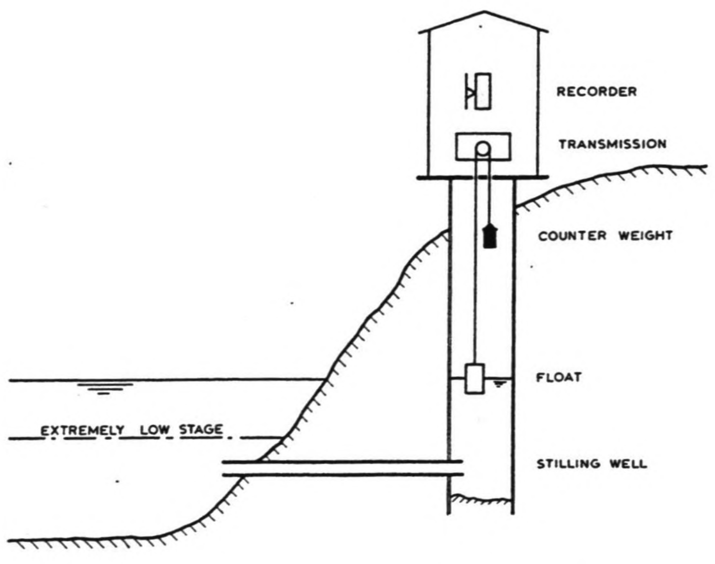

fig. 6.7 Float gauging station

The pneumatic gauge (fig. 6.5) is a pressure-measuring device. The diaphragm is placed at a fixed elevation in the stream and is connected to a manometer by a metal tube.
The electromagnetic gauge (fig. 6.6) is based on the principle of inverse echo sounding. A high frequency signal is transmitted by the oscillator and reflected by the water surface. The time interval between transmission and reception is measured and converted into a water level. The measurement takes place in a stilling well which is connected to the stream by a metal tube.
In the floating gauge (fig. 6.7) the elevation of a floating object is measured in a stilling well. A counter weight tightens the line and enables data recording.

fig. 6.8 Electric manometer

An alternative for the pneumatic gauge (fig. 6.8) is the electric manometer, to be placed at a fixed elevation in a stilling tube. The permeable tube damps the wave fluctuations and the effects of non-hydrostatic pressures caused by local accelerations. The manometer can be connected directly to a datalogger. An air tube through the cable of the manometer ensures that the air pressure is compensated.

6.3.3 The tracer-releasing device

For small-scale experiments a Mariotte Vessel (fig. 2.2) is used. The tracer release for the experiments discussed in chapter 2 was carried out using a vessel releasing 40 litres in 10 minutes (0,067 l/s). An air inlet tube inside the vessel causes a constant head, ensuring a steady vessel discharge (fig. 6.10).
For a discharge measurement during a 6-hours flood wave, with much higher river discharges, a vessel of a much larger magnitude is required. Different alternatives could be worked out. For instance, the vessel could be periodically refilled from backing tanks, or on-line mixing installations could perform a tracer release. Already existing continuous spills could be used as a tracer material (sewege outlets, factory pollutants) if well quantifiable. If the spill is not steady, it should be registered continuously. The flood-wave reconstructing procedure MINIFATS in FINDQ and DUD can handle unsteady spills and unsteady background concentrations.

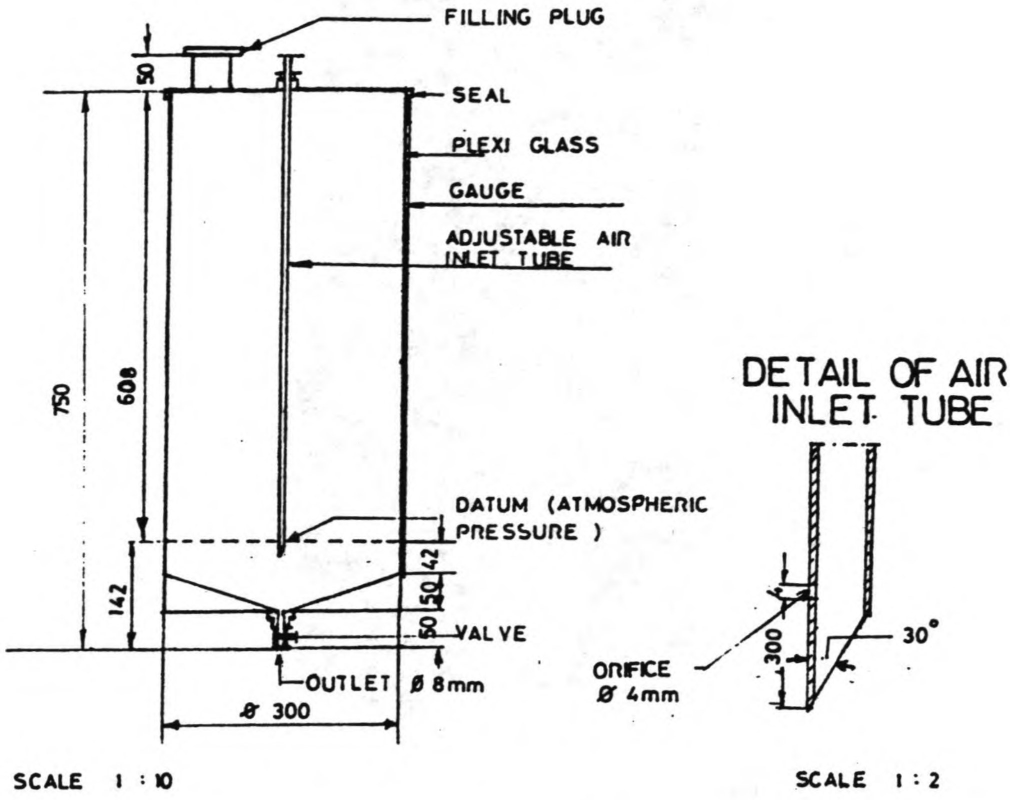

fig. 6.10 Air inlet tube in Mariotte Vessel (design: ITS Surabaya)

The exact design of the tracer releasing device depends highly on local conditions, the spill duration and the release discharge. This again depends directly on the expected maximum river discharge and the desired accuracy (2.9).

6.3.4 The datalogger

Data-recording devices develope rapidly. Analogic equipment like tape recorders and graph plotters are being replaced by digital dataloggers. A datalogger is a data-recording instrument, programmable to execute control functions.
The analogue input ports can be directly connected to the measurement equipment. The datalogger can be programmed to convert the analogue electric input signals into usable digital data and to store them on a memory card. This requires of course an accurate calibration. The memory card (upto 1 MB) is to be replaced periodically, and can be connected to a personal computer.
A few ouput ports enable control functions under programmable (for instance input dependent) criteria. Examples are:

- opening or closure of the valve under an upstream water level condition
- control of a pump to refill the vessel
- flood-wave alarm signal

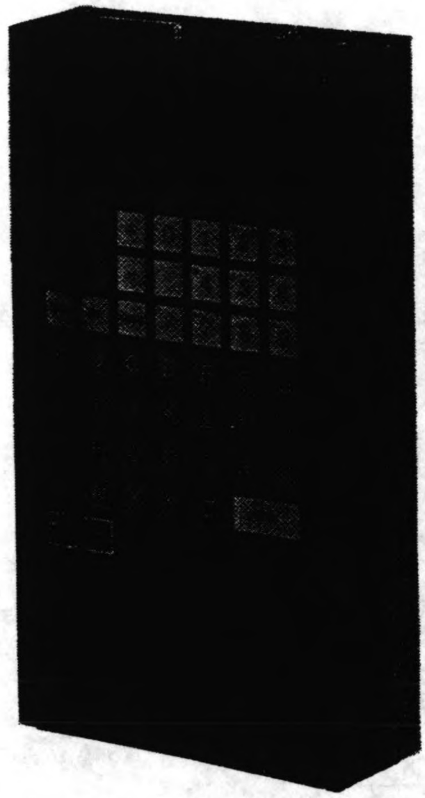

fig. 6.11 Skipper, a portable datalogger

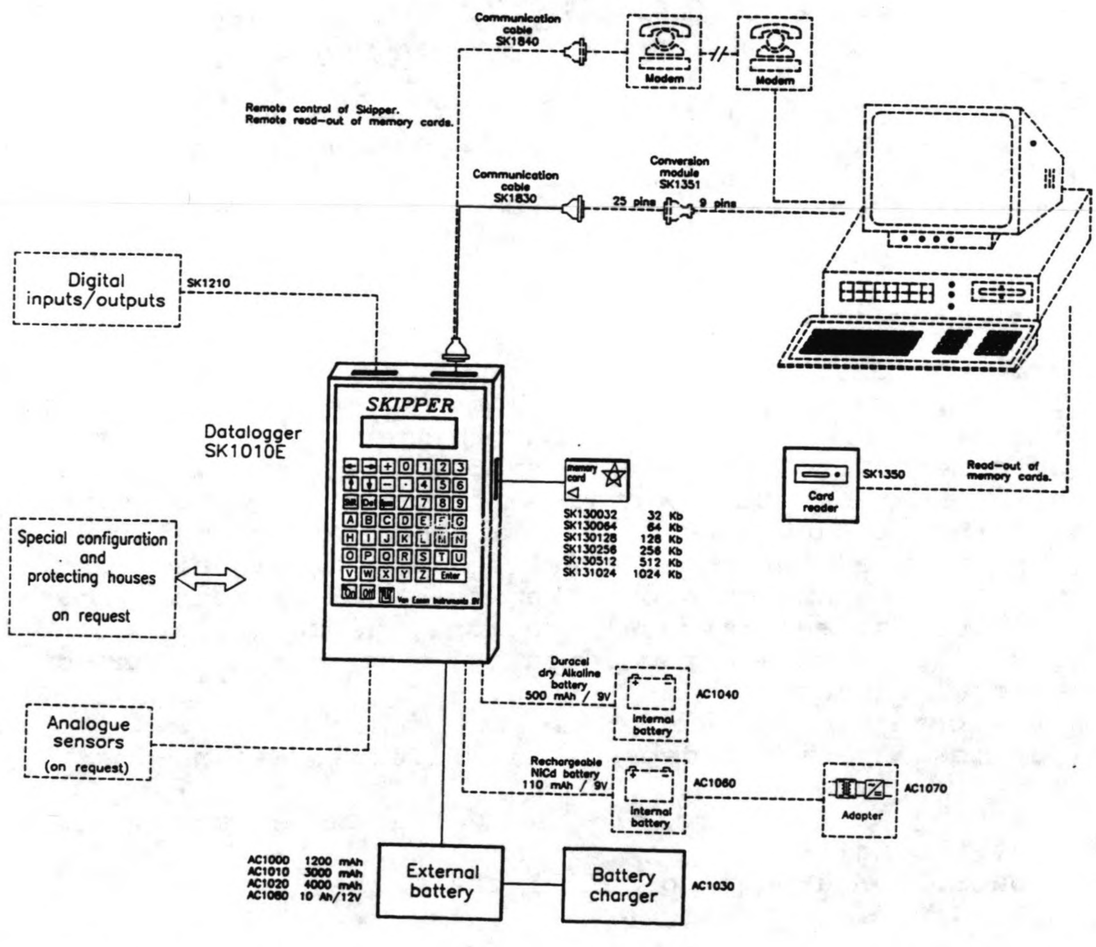

fig. 6.12 Basic configuration of the datalogger Skipper

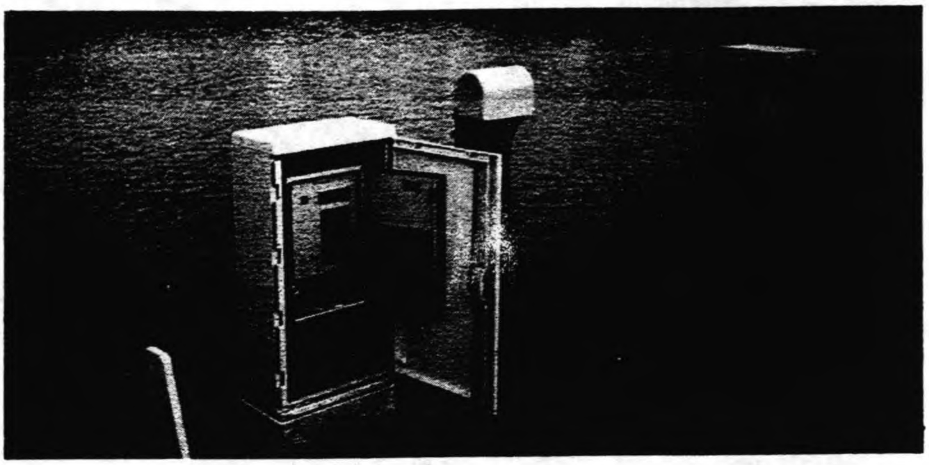

fig. 6.13 A datalogger registering observations at a river site

A few other useful applications, outside the scope of this study, can be mentioned:

- continuous water-quality observations using temperature sensors, pH-electrodes, oxigen electrodes, etc.
- observations and control functions in an irrigation network

Dataloggers are very useful, relatively cheap instruments by means of which observation and control procedures can be automised. Various versions of dataloggers exist with various possibilities, such as direct communication with personal computers or datalogger modems for communication over the telephone network (fig. 6.12).
A datalogger acts like a small portable microcomputer executing field work (fig. 6.13).

6.4 Implementation of a measurement network

If a measurement network, like the one described in this chapter, is to be implemented in a natural open channel, many factors play a role in the final design.
A good location must be found and a mixing length must be determined. The river section, hereby defined, should not contain confluences or bifurcations, nor any pollutant releases that could possibly influence the conductance of the water.
If the conditions are right, an existing continuous spill could be used as a tracer material, as discussed in the previous section.
In this chapter a few suggestions have been mentioned for the implementation of the dilution method for unsteady-discharge measurements. If the measured data, the (possibly unsteady) tracer release and the background concentration are loaded into the datafile MEASURE.MAT, the river discharge can be approximated by the computer programs FINDQ and DUD.

7. Conclusions and recommendations

The aim of this study is to develop a method to measure unsteady discharges in mountain rivers using the dilution method.

The discharge has to be determined using three continuous measurements; two water levels and a concentration. The river geometry is unknown.
The approach is the recognition of a system identification problem. Because the geometrical parameters in an irregular, boulder-studded mountain river are physically undefinable and meaningless, they must be determined by fitting the measurements into a system of flow and transport equations, with parameters to be defined. For this a DUD procedure is used. DUD is a derivative-free parameter estimation procedure based on least-squares-fitting of the observations.
This parameter estimation, improved by repeated flood wave reconstructions, results in observations that finally coincide with the measurements. The determined river discharge proves to tend towards the right solution.

Some techniques to obtain the necessary measurements are outlined. The accuracy of the result depends, just as for steady flow conditions, mainly on the accuracy of the concentration measurements and the tracer release (2.9). The error introduced by the identification procedure is difficult to quantify. However, indications show that this error is very limited if the observations fit well to the measurements.

The results show that the aim of this study has been achieved. A limitation, however, is that the flow model cannot handle internal transitions between subcritical and supercritical flow. A recommendation for further study is the development of a flow model that can deal with this problem.

Laboratory and field experiments are recommended as a topic for further study.

List of symbols

	unit
a = river depth	[m]
c = celerity	[m/s]
c_1, c_2 = short wave celerities c_r = relative numerical celerity (dimensionless)	
d = damping factor	[-]
d_n = relative numerical damping factor d_r = relative friction damping factor	
e = 2.7182818284	[-]
f = friction function in equation of motion	[m^3/s^2]
$f(\Theta)$ = system evaluation using Θ parameters	
g = acceleration due to gravity ($\approx$ 9.81 m/s^2)	[m/s^2]
h = water level	[m]
i = imaginary number (i^2=-1)	
i = integer	[m]
i = slope	[-]
i_b = bottom slope i_s = steady water surface slope	
j = integer (spatial step number)	[-]
k = disintegration factor	[s^{-1}]
k = wave number	[-]
$\ell(\alpha)$ = linear approximation of $f(\Theta)$	
m = number of grid points	[-]
n = integer	[-]
n = number of elements in Y and $f(\Theta)$ n = time step number	
p = number of elements in Θ vector	[-]
p = pressure	[N/m^2]
$\overline{p}'$ = cross-sectional averaged fluctuation p' = local fluctuation	

r = relative deviation [-]

subscript = variable referred to

r = linearised friction factor [s^{-1}]

t = time co-ordinate [s]

Δt = numerical time step

u = longitudinal flow velocity [m/s]

$\bar{u}$ = cross-sectional averaged velocity
u' = turbulent fluctuation
u'' = local deviation
u_* = bed shear velocity

v = transversal flow velocity [m/s]

v' = turbulent fluctuation

$\mathbf{v}$ = boundary condition vector

w = vertical flow velocity [m/s]

w' = turbulent fluctuation

x = longitudinal spatial co-ordinate [m]

Δx = numerical spatial step
x_p = distance between electrode plates

y = transversal spatial co-ordinate [m]

y_1, y_2 = co-ordinates of river banks

$\mathbf{y}$ = state vector

z = vertical spatial co-ordinate [m]

z_b = bottom level
z_0 = bottom level at beginning of river section
z_L = bottom level at end of river section

A = surface area [m^2]

A = cross-sectional area
A_d = cross-sectional dead-zone area
A_s = cross-sectional flow area
A_p = surface area of electrode plates

B = river width [m]

- B' = effective flow width (3.39)
- B_0 = river width at beginning of river section
- B_L = river width at end of river section
- B_s = flow width

C = Chézy coefficient [$\sqrt{m}$/s]

D = entrainment coefficient [s^{-1}]

- D_d = dead-zone entrainment coefficient
- D_s = entrainment coefficient for flow area

ΔF = matrix in DUD procedure

I = electric current [A]

J = cost function (summoned squares of errors) [-]

- $J(\Theta)$ = cost function of system evaluation using Θ
- $J_{\ell(\alpha)}$ = cost function of linearisation

K = conductivity cell constant [cm^{-1}]

K = diffusion / dispersion coefficient [m^2/s]

- K = dimensionless dispersion coefficient (2.3 and 2.4)
- K_x = longitudinal diffusion coefficient
- K_y = transversal diffusion coefficient
- K_z = vertical diffusion coefficient
- K_{num} = numerical diffusion coefficient

L = length [m]

- L = length of concentration cloud
- L = length of flood wave
- L = length of river section

L_s = specific conductance of a medium (for T=25 °C) [µS/cm]

M = system transition matrix

- M_1, M_2 = matrices in implicit numerical scheme

M = tracer release [kg/s]

P = cell-Péclet number [-]

P = wetted perimeter [m]

- P_d = exchange perimeter between main stream and dead zone

R = electric resistance [Ω]

R = hydraulic radius [m]

T = duration [s]

T = time of flood wave propagation
T = duration of flood wave
T = duration of flow processes to be computed

T = temperature [°C]

Q = river discharge [m^3/s]

Q_m = 'measured' river discharge (by dilution method using steady state formula)
Q_r = $Q(L, t)$ defined by Noppeney (1987)
Q_s = discharge, based on steady $Q(h)$ relation
Q_{ds} = exchange discharge between flow area and dead zone

U = local longitudinal flow velocity [m/s]

V = electric voltage [V]

V = local transversal flow velocity [m/s]

V_d = dead-zone volume in a river section [m^3]

W = local vertical flow velocity [m/s]

X = state of a system

X = reality
X' = computational state

Y = observation vector

Y = real measurements
Y' = computational observation

Greek

α = vector in Θ-space

α = velocity-distribution parameter [-]

ß = dead-zone fraction [-]

ε = ratio A_d/A_s [-]

Θ = parameter vector

Θ_{new} = new parameter vector, found by DUD

μ = empirical factor in dispersion coefficient [-]

μ = statistical average

subscript = variable referred to

ν = kinematic viscosity [m^2/s]

ξ = friction factor [m^{-3}]

ξ = relative grid size [-]

π = 3.1415926536 [-]

ρ = specific density of medium (water) [kg/m^3]

ρ = numerical amplification factor (complex) [-]

σ = Courant number [-]

σ = standard deviation

subscript = variable referred to

τ = shear stress [N/m^2]

$\overline{\tau_b}$ = cross-sectional averaged bottom stress
τ_b = local bottom stress
τ_{xy} = shear stress in *xy*-plane of water particle
τ_{xz} = idem in *xz*-plane
τ_{yz} = idem in *yz*-plane

ϕ = concentration [kg/m^3]

ϕ' = fluctuation
ϕ'' = local deviation
ϕ_d = mean concentration in dead zone

ω = empirical factor in entrainment coefficient [-]

$\boldsymbol{\Theta}$ = weighing factor in implicit numerical scheme [-]

$\Delta\boldsymbol{\Theta}$ = matrix in DUD procedure, containing p+1 Θ-vectors

Φ = local concentration [kg/m^3]

References

Chavent G. (1985)
Identification of distributed parameter systems: about the output least square method, its implementation and identifiability
University of Paris, IX-Dauphine

Chen Han-Fu (1989)
Identification and system parameter estimatión 1988
IFAC Proceedings, series 1989 No. 8

Geer F.C. van (1981)
Inleiding Kalmanfilter (hydrologische toepassingen)
TU Delft, faculty of Civil Engineering

ISO Standards Handbook 16 (1983)
Measurements of liquid flow in open channels
International Organization for Standardization

Fischer, H.B. et al. (1974)
Mixing in inland and coastal waters
Academic Press, New York

Jansen P. et al. (1979)
Principles of river engineering
Pitman, London

MathWorks Inc. (1985)
PC-Matlab User's Guide
MathWorks Inc., Portola Valley, California

Natke H.G. (1988)
Application of system identification in engineering
Springer-Verlag, Wien-New York

Noppeney, R.M. (1987)
Applicability of dilution discharge measurements during flood wave conditions, Thesis
TU Delft, Faculty of Civil Engineering

Nordin C.F. and Troutman B.M. (1980)
Longitudinal dispersion in rivers: The persistence of skewness in observed data
Water Resources Research, vol.16, no.1

Purnama A. (1988)
The effect of dead zones on longitudinal dispersion in streams
Journal of Fluid Mecanics, vol.186

Ralston M.L. and Jennrich R.I. (1978)
DUD, a derivative free algorithm for nonlinear least squares
Technometrics, vol.20, no.1

Sofia F. and Sholeh M. (1990)
Design of Mariotte Vessel for discharge measurements using dilution method
ITS Surabaya, Faculty of Civil Engineering

Valentine E.M. and Wood I.R. (1977)
Longitudinal dispersion with dead zones
Journal of the Hydraulics Division, vol.103, no.Hy9

Verspuy C. (1987)
Lange golven (lecture notes b73)
TU Delft, Faculty of Civil Engineering

Vreugdenhil, C.B. (1985)
Numerieke berekeningen in waterbouwkunde en hydrologie (lecture notes b84)
TU Delft, Faculty of Civil Engineering

Vreugdenhil, C.B. (1989)
Computational Hydraulics, an Introduction
Springer-Verlag, Berlin

Vries, M. de (1986)
Rivierwaterbouwkunde (lecture notes f13B)
TU Delft, Faculty of Civil Engineering

Vries, M. de (1990)
Transport processes in open channels
TU Delft / ITS Surabaya, Faculties of Civil Engineering

Vroege P. (1991)
Dilution method for measurement of unsteady flow using back-into-time Kalman filtering, Thesis
TU Delft, Faculty of Civil Engineering

Commercial documentation from (1991):
Schott Geräte GmbH
Van Essen Instruments BV
Yellow Springs Instruments Co., Inc.

920583